New refined Model for Mechatronics design of solar mobile robotic platforms

Farhan A. Salem

Abstract—This paper proposes a new generalized and refined model for Mechatronics design of Solar Electric Mobile Robotic Platforms (SEMRP) and some considerations regarding design, modeling and control solutions. The proposed models are developed to help in facing main challenges in developing Mechatronics mobile robotic systems, in particular; early identifying system level problems and ensuring that all design requirements are met, and developed to allow designer to have the maximum output data to to select, design, tested and analyze overall SEMRP system and each subsystem outputs characteristics and response, for desired overall and/or either subsystem's specific outputs, under various PV subsystem input operating conditions, to meet particular SEMRP system requirements and performance. The proposed SEMRP system model consists of five main subsystems, each subsystem is mathematically described and corresponding Simulink sub-model is developed, then an integrated model of all subsystems is developed, tested and evaluated for desired system requirements and performance, the obtained results show the simplicity, accuracy and applicability of the presented models in Mechatronics design of SEMRP system applications, as well as, for application in educational process.

Index Terms—Mechatronics, Solar Electric Mobile Robotic Platform (SEMRP), PV Panel, Modeling/simulation.

1. INTRODUCTION

The essential characteristic and the key to success in Mechatronics design is a balance between two sets of skills modeling/analysis and experimentation / hardware implementation skills. Modeling, simulation, analysis and evaluation processes in Mechatronics design consists of two levels, sub-systems models and whole system model with various sub-system models interacting similar to real situation, the subsystems models and the whole system model, are tested and analyzed for desired system requirements and performance [1].

Mobile robot is a platform with a large mobility within its environment (air, land, underwater) it is not fixed to one physical location. Mobile robots have potential application in industrial and domestic applications. Generally, Mobile robots are a relatively new research area that is not normally considered from several different perspectives. Different researches on Mobile robots fundamentals, mathematical and Simulation models can be found including but not limited to in [1-22], most of it study separate specific system or subsystem design, dynamics analysis, control or application. Solar electric mobile platform (SEMRP) system is relatively new field of mobile robots and new research area, a generalized refined model of overall SEMRP system that can represent the actual system dynamics and that can be used in Mechatronics mobile robotic system design is of concern.

Farhan A. Salem is currently with Taif University Saudi Arabia. Dept. of Mechanical Engineering, Mechatronics engineering prog., College of Engineering, and Alpha center for Engineering Studies and Technology Researches, Amman, Jordan. Email: salem_farh@yahoo.com

One of the simplest and most used structures in mobile robotics applications, are the two-wheel differential drive mobile robots shown in Fig. 1, it consists of a chassis with two fixed and in-lines with each other electric motors and usually have one or two additional third (or forth) rear wheel(s) as the third fulcrum, in case of one additional rear wheel, this wheel can rotate freely in all directions, because it has a very little influence over the robot's kinematics, its effect can be neglected [12]. Accurate designing and control of mobile robot is not a simple task in that operation of a mobile robot is essentially time-variant, where the operation parameters of mobile robot, environment and the road conditions are always varying, therefore, the mobile robot as whole including controller should be designed to make the system robust and adaptive, improving the system on both dynamic and steady state performances. To help in facing the two top challenges in developing Mechatronics systems; early identifying system level problems to optimize system level performance to meet the design requirements and ensuring that all design requirements are met, as well as, while maintaining desired accuracy, to simplify and accelerate Mechatronics design process of mobile robots, including proper selection, analysis, integration and verification of the overall system and sub-systems performance throughout the development process, this paper extends writer's previous works [15-16] [23-27] and proposes new generalized and refined model for Mechatronics design of SEMRP system, the proposed model is to be developed to allows designer to have the maximum output data to select, integrate, tested and analyze the SEMRP system for desired overall and/or either subsystem's outputs under various PV system operating conditions, to meet particular SEMRP system requirements. The proposed SEMRP system and its block diagram representation are shown in Fig. 1(a)(b), the SEMRP system consists of five main subsystems including; PV panel, DC/DC converter, mobile platform, actuator, control unit , each subsystem, to be mathematically described and corresponding Simulink sub-model developed , then an integrated design of all subsystem is to be developed, the subsystems models and the whole SEMRP system model, are to be tested and analyzed for desired system requirements and performance

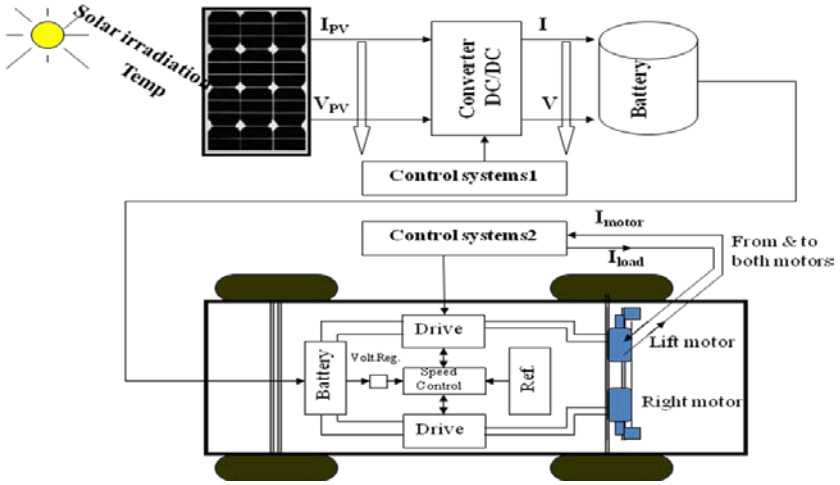

Fig. 1(a) The block diagram of proposed SEMRP system configurations and control

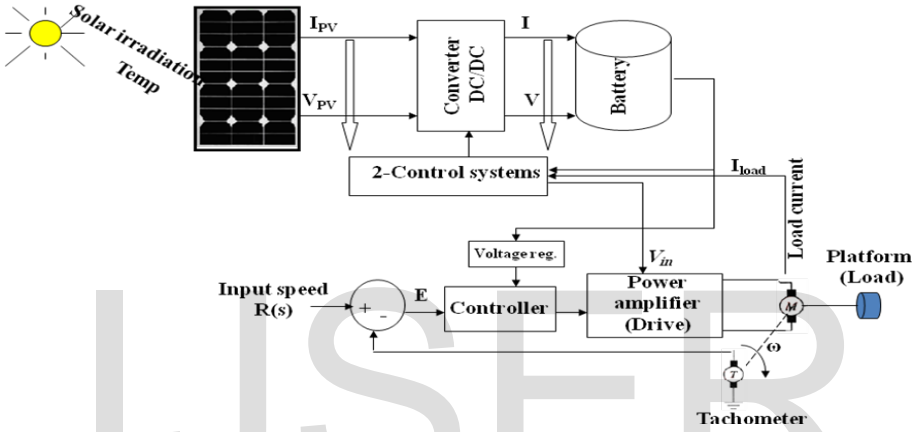

Fig. 1(b) The block diagram of proposed SEMRP system configurations and control

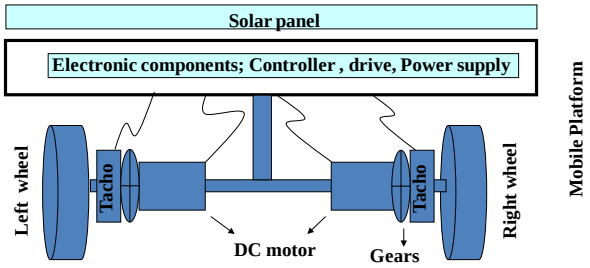

Fig. 1(c) Solar electric mobile robotic platform (SEMRP) system

2. SEMRP system modeling

The proposed SEMRP system and block diagram representation is shown in Fig. 1(a)(b), it consists of five main subsystems including; PV panel, DC/DC converter, mobile platform, DC machine and control unit subsystems, each subsystem, each subsystem is to be mathematically described and corresponding Simulink sub-model developed, then an integrated generalized design of overall SEMRP system of integrated subsystems will be developed, to result in generalized SEMRP system, the subsystems models and the whole SEMRP system model, are to be tested and analyzed for desired system requirements and performance.

2.1 Modeling of mobile platform

A detailed description, fundamentals, mathematical and Simulink models of mobile robots can be found in different resources, most of it study separate specific system or subsystem design, dynamics analysis or control, including [1-22]. In [14] Proposes a new refined mathematical, Simulink and function block models for mobile robots and some considerations regarding Mechatronics design and control solutions are proposed and tested. In [15] Mechatronics design of electric machine and corresponding motion control in terms of desired output position or velocity, for desired *deadbeat response* specifications are proposed and tested, the proposed design can be used for different Mechatronics motion control design application where the proper selection of actuating machine and design of precise motion control system are of concern, the design can be simplified, accelerated and evaluated, using both or either of proposed new MATLAB built-in function named *deadbeat( )*. In [16] mathematical and Simulink models of mobile robot in the form of wheeled chair are proposed and

controlled to achieve desired output performance and speed. In [18] dynamic analysis and control of mobile robots using a proposed generalized model are proposed. In [19] Design and implementation of an experimental mobile robotic system is proposed, a model of designed robot was created in environment of the ADAMS simulation software and the electrical drive system was modeled in the Simulink software, the obtained data was used in the process of determination of appropriate driving motor, moreover, the real experiments with constructed robot were accomplished in order to verify the performed simulations. In [20] proposed models that be used for simulation and control of mobile platforms, the proposed models take into account the hardware limitations, friction force and the topography of the environment for out door navigation. In [21] Introduced modeling of power components and computer simulation as a tool for conducting transient and control studies of mobile robots. In [22] some considerations regarding mathematical models and control solutions for two-wheel differential drive mobile robots, where the closed loop control diagrams for position control and respectively for direction control in tracking along imposed trajectories are developed, analyzed and included.

2.1.1 Actuator subsystem modeling

In order to drive a SEMRP, induction motors, reluctance and permanent magnet motors can be used, the actuating machines most used in Mechatronics motion control applications are PMDC machines (motors).In this paper, PMDC motor is considered as SEMRP electric actuator, based on this, the SEMRP system motion control can be simplified to a PMDC machine motion control. depending on application requirements, any other actuating machine can also be used to replace PMDC motor to develop a generalized model.

Considering that the DC motor subsystem dynamics and disturbance torques depend on mobile platform shape and dimensions, in modeling DC motors and in order to obtain a linear model, the hysteresis and the voltage drop across the motor brushes is neglected, other DC motors types can be used, where the input voltage, V_{in} maybe applied to the field or armature terminals [28].

A detailed mathematical description and Simulink models of DC machine has been studied for last decades, and can be found in different resources including; [12-17][26-27][29].

In [16-17] a detailed derivation of DC machine and mobile robotic platform mathematical and Simulink models are derived and developed, as well as, function block with its function block parameters window, based on these references, the DC motor system dynamics are expressed as given by Eq.(1),The coulomb friction can be found at steady state, *to be* as by Eq.(2).Since the open loop transfer function of SEMRP system is simplified to DC motor open loop transfer function, the equivalent SEMRP system open loop transfer function with load and gears attached, in terms input voltage, $V_{in}(s)$, and shaft output angular velocity, $\omega(s)$, is given by Eq.(3).The geometry of the mechanical part determines the moment of inertia, the SEMRP system can be considered to be of is cylindrical shape ⊏⎯, with the inertia calculated as given by Eq.(4) , where the total equivalent inertia, J_{equiv} and total equivalent damping, b_{equiv} at the armature of the motor with gears attaches, are given by Eq.(5). The inertias of the gears and wheels have to be included in the calculations of total equivalent inertia, as by Eq.(5)

$$K_t\, i_a = T_\alpha + T_\omega + T_{load} + T_f \tag{1}$$

$$K_t\, i_a - b^*\omega = T_f \tag{2}$$

$$G_{speed}(s) = \frac{\omega_{platform}(s)}{V_{in}(s)} = \frac{K_t / n}{\left[(L_a J_{equiv})s^2 + (R_a J_{equiv} + b_{equiv} L_a)s + (R_a b_{equiv} + K_t K_b)\right]} \tag{3}$$

$$b_{equiv} = b_m + b_{Load}\left(\frac{N_1}{N_2}\right)^2 \Leftrightarrow J_{equiv} = J_m + J_{Load}\left(\frac{N_1}{N_2}\right)^2 \qquad J_{load} = \frac{bh^3}{12} \Leftrightarrow J_{equiv} = J_{motor} + J_{gear} + (J_{wheel} + mr^2)\left(\frac{N_1}{N_2}\right)^2 \tag{4}$$

In the following calculation the disturbance torque, T, is all torques including coulomb friction, and given by $(T=T_{load}+T_f)$, and correspondingly, the open-loop transfer function of the PMDC is given by Eq.(5). Based on Eq. (3), two Simulink models of DC machine subsystem shown in Fig. 2(a)(b) are developed , these sub-models will be used in this paper to represent DC machine sub-model..

$$G_{open}(s) = \frac{\omega_{platform}(s)}{V_{in}(s)} = \frac{K_t / n}{(L_a s + R_a)(J_{equiv} s^2 + b_{equiv} s) + (L_a s + R_a)(T) + K_b K_t} \tag{5}$$

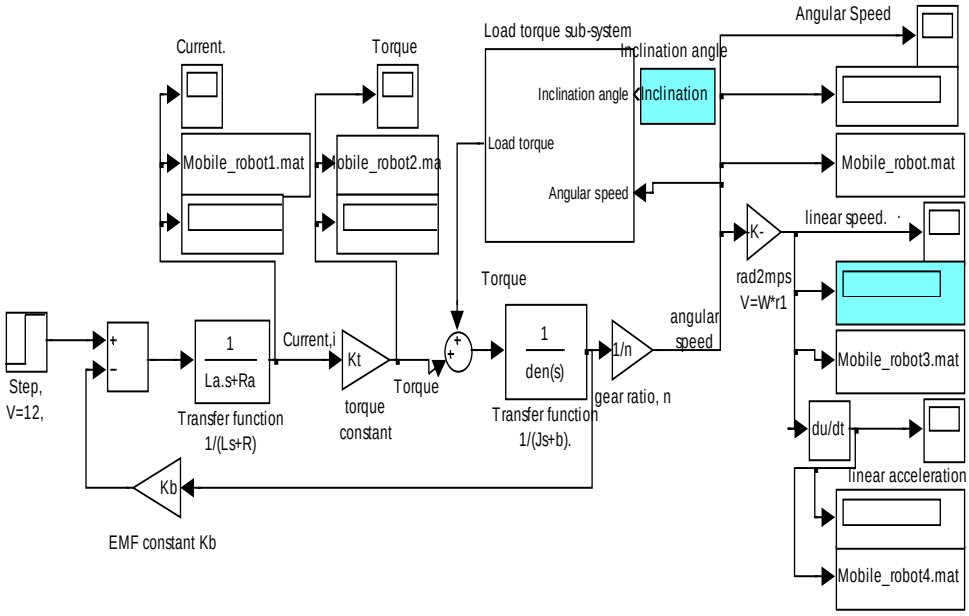

Fig. 2(a) DC machine sub-model in Simulink

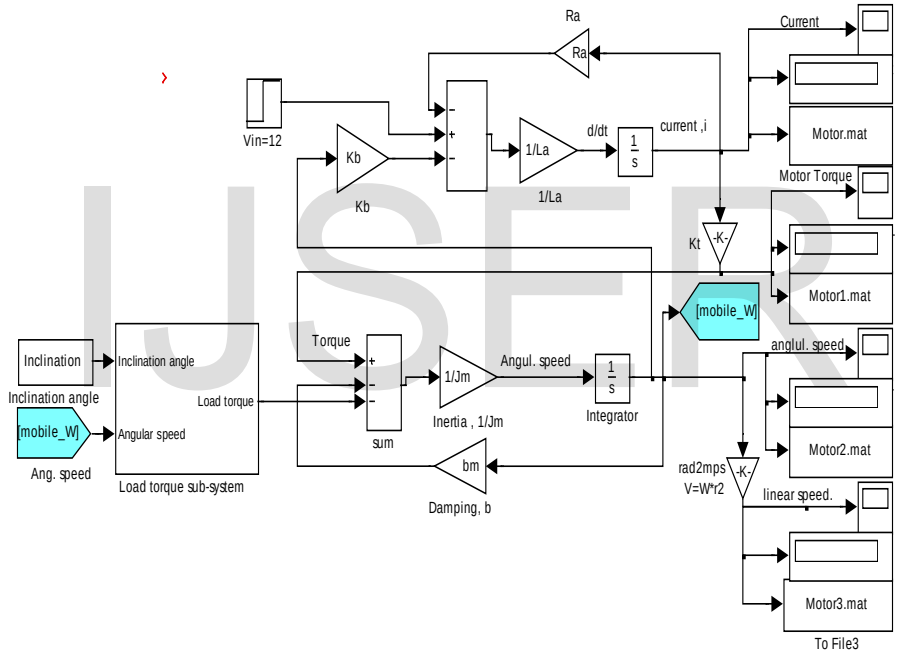

Fig. 2(b) DC machine sub-model in Simulink

Fig. 2(a)(b) open loop Simulink model of DC machine subsystem sub-model with load torque

2.1.2 Modeling of SEMRP platform dynamics.

In [14] is introduced a detailed derivation of refined mobile platform mathematical and Simulink models including most possible acting forces, tested and verified. Several forces are acting on mobile platform when it is running, the modeling of a mobile platform system dynamics involves the balance among the acting on a running platform forces, and these acting forces are categorized into road-load and tractive force. The road-load force consists of the gravitational force, rolling resistance of the wheels, the aerodynamic drag force and the aerodynamics lift force. The resultant force is the sum of all these acting forces, will produce a counteractive torque to the driving motor, i.e., the tractive force. The disturbance torque to mobile platform is the total resultant torque generated by the acting forces, and given by Eq.(6).The driving force comes from the powertrain shaft torque, which can be written as the wheel torque, given by Eq.(7), This wheel torque provides the resultant driving, tractive force, F_T to the platform, and referring to Fig. 3, the relationship between the resultant tractive force and the torque produced by the motor T_s ,can be obtained as shown in Eq.(8) .The platform inertia torque can be defined by Eq.(9). It is required to couple the mobile platform with the wheel rotational velocity via characteristics of the electric motor and surface such as the traction force, the torque, etc. The relationship between the linear velocity of the platform,

v, and the angular velocity of the electric motor is given by Eq.(10):

$$F_{Total} = \mathrm{F_a} + \mathrm{F}_R + \mathrm{F}_C + \mathrm{F_{Lin\_a}} + F_{ang\_a} \quad (6)$$

$$T_{wheel} = n\eta T_{shaft} \quad (7)$$

$$F_{Total} = \frac{T_{wheel}}{r} = \frac{n\eta T_{shaft}}{r}, \quad \Rightarrow T_{shaft} = F_{Total}\frac{r}{n\eta} \quad (8)$$

$$T = J_{Vehicl}\frac{d\,\omega_{vehicl}}{dt} \quad (9)$$

$$\upsilon = \frac{r_{wheel} * \omega}{n} \quad (10)$$

To determine the electric battery capacity, and correspondingly design of the Photovoltaic panel with series and parallel connected cells, it is required to estimated energy required by platform, the required power in kW that platform must develop at stabilized speed can be determined by multiplying the total force with the velocity of the SMEV, and given by Eq.(11):

$$P_{Total} = (\sum F) * \upsilon = F_{Total} * \upsilon \quad (11)$$

Electrical power (in watts) in a DC circuit can be calculated by multiplying current in Amps and V is voltage, and given by Eq.(12).Based on fundamental principle of dynamics the acceleration of the vehicle is given by Eq.(12):

P= I x V (12)

$$\alpha = \frac{P_m - P_{total}}{M * \upsilon} \quad (13)$$

The driving force comes from the powertrain shaft torque, which can be written as the wheel torque, given by Eq.(7). This wheel torque provides the resultant driving, tractive force, F_{Total} to the vehicle and given by Eq.(14):

$$F_{Total} = \frac{T_{wheel}}{r_{wheel}} = \frac{n * \eta * T_{shaft}}{r_{wheel}} \quad (14)$$

Referring to Fig. 3, the relationship between the resultant tractive force and the torque produced by the motor T_{shaft} ,can be obtained as by Eq.(15):

$$T_{shaft} = F_{Total} * \frac{r_{wheel}}{n * \eta} \quad (15)$$

The platform inertia torque can, also, be defined by relationship given by Eq.(16):

$$T = J_{platform}\frac{d\,\omega_{platform}}{dt} \quad (16)$$

When modeling mobile platform, considering desired accuracy and platform system dimensions, the following most acting forces and corresponding torques, can be considered:

The rolling resistance force,

$$\mathrm{F_{rolling}} = F_{normal\_force}\mathrm{C_r} = Mg\mathrm{C_r}\cos(\alpha) \quad (17)$$

For motion on a level surface, $\alpha=0$, $\cos(\alpha)=1$, and Eq.(17) becomes:

$$\mathrm{F_{rolling}} = F_{normal\_force}\mathrm{C_r} = Mg\mathrm{C_r} \quad (18)$$

In terms of the vehicle linear speed Eq.(17) becomes:

$$\mathrm{F_{rolling}} = \mathrm{M\ g}\left(\mathrm{C_{r0}} - \mathrm{C_{r1}} * \upsilon\right) sign(\upsilon) \quad (19)$$

The rolling resistance coefficient C_r ,is calculated by expression given by Eq.(20):

$$\mathrm{C_r} = 0.01\left(1 + \frac{3.6}{100}\upsilon_{robot}\right) \quad (20)$$

The rolling resistance torque is given by Eq.(21)

$$\mathrm{T_{rolling}} = \left(Mg\mathrm{C_r}\cos(\alpha)\right) r_{wheel} \quad (21)$$

The **hill-climbing resistance force** is given by Eq.(22):

$$\mathrm{F_{climb}} = \mathrm{F_{slope}} = \left(Mg\sin(\alpha)\right) \quad (22)$$

The hill-climbing resistance, *slope*, torque, is given by Eq.(23):

$$\mathrm{T_{climb}} = \mathrm{T_{slope}} = \left(Mg\sin(\alpha)\right) r_{wheel} \quad (23)$$

The **total inertia force** of the mobile platform , is given by Eq.(24),The inertia torque is given by Eq.(25):

$$F_{inertia} = F_{slope} = M\frac{d\,v}{dt} \quad (24)$$

$$T_{inertia} = T_{slope} = \left(M\frac{d\,v}{dt}\right)\left(r_{wheel}\right)^2 \quad (25)$$

The **Aerodynamic Drag force**, given by Eq.(26),Considering car and wind speed Eq.(26) become:

$$\mathrm{F_{aerod}} = 0.5\rho\mathrm{AC_d}\upsilon_{vehicl}^2 \quad (26)$$

$$\mathrm{F_{aerod}} = 0.5\rho\mathrm{AC_d}\left(\upsilon_{vehicle} + \upsilon_{wind}\right)^2 sign(\upsilon_{vehicle})$$

$$\mathrm{F_{aerod}} = 0.5\rho\mathrm{AC_d}\left(\upsilon_{vehicl} + \upsilon_{wind}\right)^2 sign\left(\upsilon_{vehicl} + \upsilon_{wind}\right)$$

The aerodynamics torque is given by Eq.(27).The aerodynamic drag coefficient C_d : characterizing the shape of the SMEV and can be calculated using expression, given by Eq.(28):

$$\mathrm{T_{aerod}} = \left(\frac{1}{2}\rho\mathrm{AC_d}\upsilon_{vehicle}{}^2\right) r_{wheel} \quad (27)$$

$$C_D = \frac{\mathrm{F_{aerod}}}{0.5\rho\upsilon^2 S} \quad (28)$$

The aerodynamics lift force, F_{lift}; given by Eq.(29).The coefficient of lift C_L, with values (C_L to be 0.10 or 0.16), can be calculated using expression given by Eq.(30):

$$F_{lift} = 0.5\rho C_L B\upsilon_{vehicle}^2 \quad (29)$$

$$C_L = \frac{L}{0.5\rho\upsilon^2 A} \quad (30)$$

The force of wind , F_{wind} ; can be calculated by Eq.(31):

$$\mathrm{F_{wind}} = 0.5\rho\mathrm{AC_d}\left(\upsilon_{vehicle} + \upsilon_{wind}\right)^2 \quad (31)$$

The angular acceleration force , is the force required by the wheels to make angular acceleration and is given by Eq.(32):

$$\mathrm{F_{acc\_angle}} = J\frac{G^2}{r_{wheel}^2}a \quad (32)$$

The angular acceleration torque is given by Eq.(33):

$$T_{acc\_angle} = \left(J\frac{G^2}{r_{wheel}^2}a\right) r_{wheel} = J\frac{G^2}{r_{wheel}}a \quad (33)$$

The linear acceleration force F_{acc} : is the force required to increase the speed of the SMEV and can be described as a linear motion given by Eq.(34):

$$F_{acc} = M * a = M \frac{d\upsilon}{dt} = \left(M + \frac{J_{wheel}}{r^2} \right) \frac{d\upsilon}{dt} \qquad (34)$$

$$F_{acc} = M * a = M \frac{d\omega}{dt} = M \frac{\sum T}{J}$$

Substituting derived equations in total force equation, we have, expression given by Eq.(35):

$$F_{Total} = \left[Mg \sin(\alpha) \right] + \left[M\, g \left(C_{r0} - C_{r1} * \upsilon \right) sign(\upsilon) \right] + \left[0.5 \rho A C_d \left(\upsilon_{vehicl} + \upsilon_{wind} \right)^2 sign\left(\upsilon_{vehicl} + \upsilon_{wind} \right) \right] + F_{Linear\_acc} + \left[\left(M + \frac{J_{wheel}}{r^2} \right) \frac{d\upsilon}{dt} \right] \qquad (35)$$

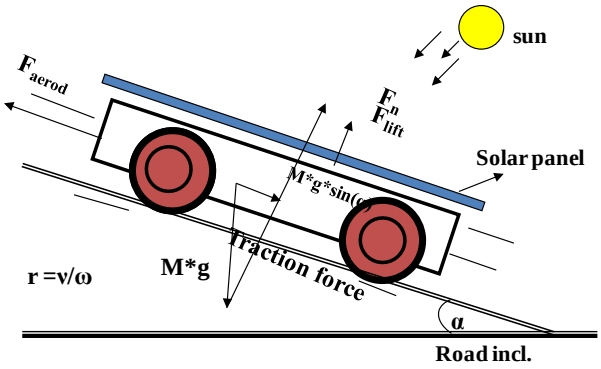

Fig. 3 Forces acting on moving solar electric mobile robotic platform.

Considering shape of mobile platform as cylinderical ⊏, the aerodynamic drag coefficient is found from aerodynamic force as follows,: the drag force is found by $F_a = \tau_m * A$, where : τ_m :shear stress and found by equation $\tau_m = \mu \left(du / dy \right)|_{y=0}$. Where: μ: air dynamic viscosity 1.5×10^{-5} . A: frontal area of platform (A=*0.58*0.92=0.5336m²*). ν: The linear speed of the mobile platform (0.5 *m/s*), substituting and calculating we find Aerodynamic drag coefficient C_d =0.80,C_d is not an absolute constant for a given body shape, it varies with the speed of airflow (or more generally with Reynolds number R_e. ν_o : The speed of the wind (*m/s*), against the direction of the platform's motion, r: wheel radius *0.075 m*. ρ: The air density (*kg/m³*) at STP, ρ =1.25, At 20°C and 101 *kPa*, ϱ =1.2041,

The air density is calculated by below expression, where: ρ_o = 101325 *Pa*, sea level standard atmospheric pressure, T_0 = 288.15 *K* sea level standard temperature. *G* = 9.81 m/s². Earth-surface gravitational acceleration. *L* = 0.0065 *K/m* temperature lapse rate. *R* = 8.31447 *J/(mol*K)* universal gas constant. *M* = 0.0289644 *kg/mol* molar mass of dry air.

$$\rho = \frac{M_o * \rho_0 \left(1 - \frac{L * h}{T_O} \right)^{\frac{g * m}{R * L}}}{R * T}$$

Load torque modeling and simulation; In [14], based on application and platform size, a detailed derivations of different models of mobile robotic platform and corresponding Simulink models, are developed. Based on derived equation the maximum calculated load torques, for the mobile robot to overcome, is simulated in Simulink refined load-torque sub-model and mask shown in generalized model shown in Fig.7 , based on desired accuracy and application other representations can be developed including shown in Fig. 4(a)(b)(c)(d), where three versions of load torque are proposed, *first* model of acting forces and corresponding torques shown Fig. 4(a) and second *simplified* model for mobile platform of medium size applications shown Fig. 4(b), in this model, the following forces can be included; the hill-climbing resistance force $F_{climb,}$ aerodynamic Drag force , F_{aerod} and the linear acceleration force F_{acc}, and to be given by Eq.(36). The load torque can be further simplified to include the total inertia force of the mobile platform, the total weight component of the robot, and the total friction force between the wheels and the topography's surface with the viscous rolling friction coefficient the corresponding Simulink sub-models is shown in Fig. 4(c). The input to load-torque sub-model is shaft angular speed *ω*, the motor torque $K_t * I_a$ for coulomb friction calculations and changes in the road surface, inclination angle, *α* as a disturbance introduced to the system.

$$F = 0.5 \rho A C_D \upsilon^2 + Mg \sin(\alpha) + m \frac{d\upsilon}{dt} \qquad (36)$$

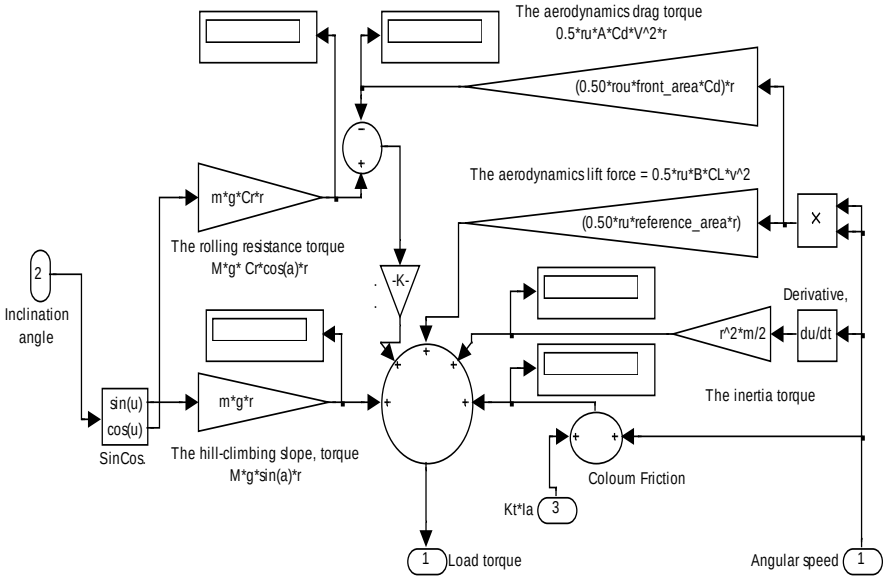

Fig. 4(a) load torque refined Simulink model

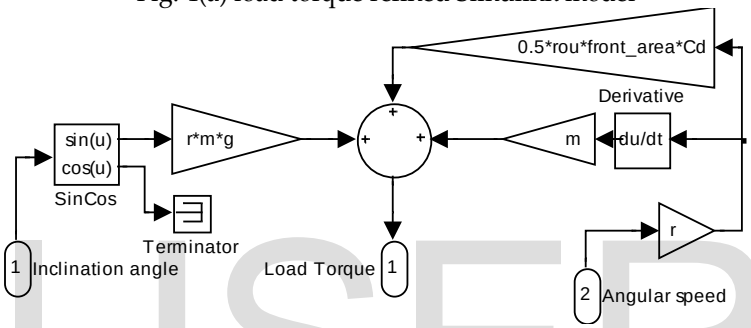

Fig. 4(b) load torque of medium size and accuracy platform model

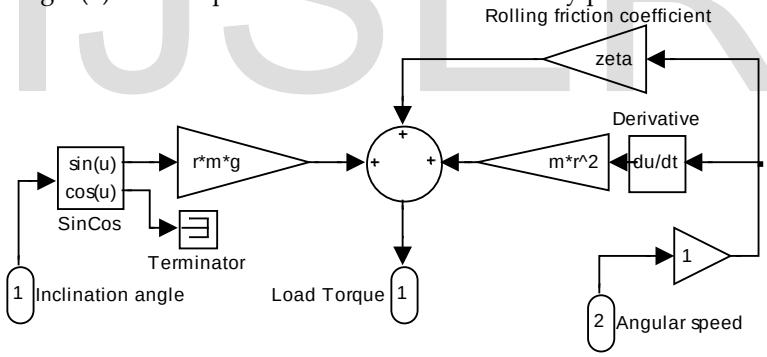

Fig. 4(c) The simplified load torque of platform model

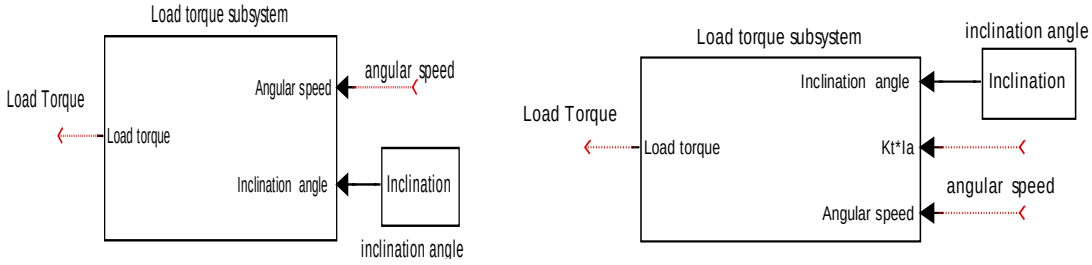

Fig. 4(d) Simulink model load torque mask

2.2 Sensor subsystem modeling

Tachometer is a sensor used to measure the actual output angular speed, ω_L. Dynamics of tachometer can be represented using Eq.(37), assuming the SEMRP system, is to move with linear velocity of *0.5 m/s*, the angular speed is obtained as shown by Eq.(38). Therefore, the tachometer constant, for calculated angular speed ω, is given as shown by Eq.(38), any other desired platform output speed can be choosing based on this approach, for example for output linear speed of 0.5m/s , ω *=0.5/0.075=6.667* and K_{tach} *=12/6.667=1.8*

$$V_{out}(t) = K_{tach}\frac{d\theta(t)}{dt} \Rightarrow V_{out}(t) = K_{tach}\omega \Rightarrow K_{tach} = \frac{V_{out}(s)}{\omega(s)} \quad (37)$$

$$\omega = \frac{v}{r} = \frac{1}{0.075} = 13.3333 \text{rad/s} \quad \Rightarrow K_{tach} = \frac{12}{13.3333} = 0.9 \quad (38)$$

2.3 Generalized Photovoltaic Panel –Converter (PVPC) subsystem model

The PV panel is used as electricity generator to convert the irradiance from sunlight into electricity using photovoltaic system to generate its own power for propulsion and for storing in batteries, and use power converter as a device that converts electrical energy source with variable needs of the electric vehicle by

switching devices .The PV Panel-Converter (PVPC) system consists of two main subsystems; PV panel and DC/DC buck converter with battery subsystems.

The PVPC system consists of two main subsystems; PV panel and DC/DC converter with battery subsystems, each subsystem will be separately, mathematically modeled and simulated in MATLAB/Simulink, and then an integrated generalized and refined model that returns the maximum output data, for design and analysis, will be developed and tested. The generalized mathematical and Simulink Photovoltaic Panel –Converter (PVPC) subsystem model and sub-models, considered in this paper are d in reference to [24-25].

2.3.1 Photovoltaic cell-Panel subsystem modeling

A general mathematical description of a PV cell in terms of output voltage, current, power and of I-V and P-V characteristics has been studied for over the past four decades and can be found in different resources, many of which are listed in [24]. ***The output net current of PV cell I***, and the V-I characteristic equation of a PV cell are given by Eq.(39), it is the difference of three currents; the light-generated *photocurrent* I_{ph}, *diode* current I_d and the *shunt* current I_{RSH} . The output voltage, current and power of PV array vary as functions of solar irradiation level β, temperature T , cell voltage V and load current I, where with *increase* in temperature at *constant* irradiation, the power output *reduces*, also, by increasing operating temperature, the current output increases and the voltage output reduces, similarly with irradiation. Therefore the effects of these three quantities must be considered in the design of PV arrays so that any change in temperature and solar irradiation levels should not adversely affect the PV array output to the load/utility [24]

$$I = I_{ph} - I_d - I_{RSH}$$

$$I = I_{ph} - I_s\left(e^{\frac{q(V+IR_S)}{NKT}} - 1\right) - \frac{V + R_S I}{R_{sh}} \quad (39)$$

$$I = \left(I_{sc} + K_i\left(T - T_{ref}\right)\right)\frac{\beta}{1000} - I_s\left(e^{\frac{q(V+IR_S)}{NKT}} - 1\right) - \frac{V + R_S I}{R_{sh}}$$

The generalized mathematical and Simulink models of PV cell, considered in this paper are built in reference to [25-26], the modified model and mask are shown in Fig. 5(a)(b), as shown, this generalized PV cell- array model is designed to allow designer to have maximum numerical visual and graphical data to select, design and analyze a given PV system for desired output performance and characteristics under given operation condition, including; cell's-panels current, voltage, powers, efficiency and fill factor. Running model given in Fig. 5(d), for PV parameters defined in Table 1, at *standard* operating conditions of irradiation β*=1000*, and *T=25*, will result in P-V and I-V characteristics shown in Fig. 5(c)(d) and shown visual numerical values of cell's-panels current, voltage, powers, efficiency and fill factor, these curves show that, this is 3.926 Watt PV cell with I_{SC} *= 8.13 A* , *Vo= 0.6120V* , I_{max} *=7.852 A* , V_{max} *=0.5 V, (MPP =* I_{max} * * V_{max} *=7.852 *0.5=3.926).*

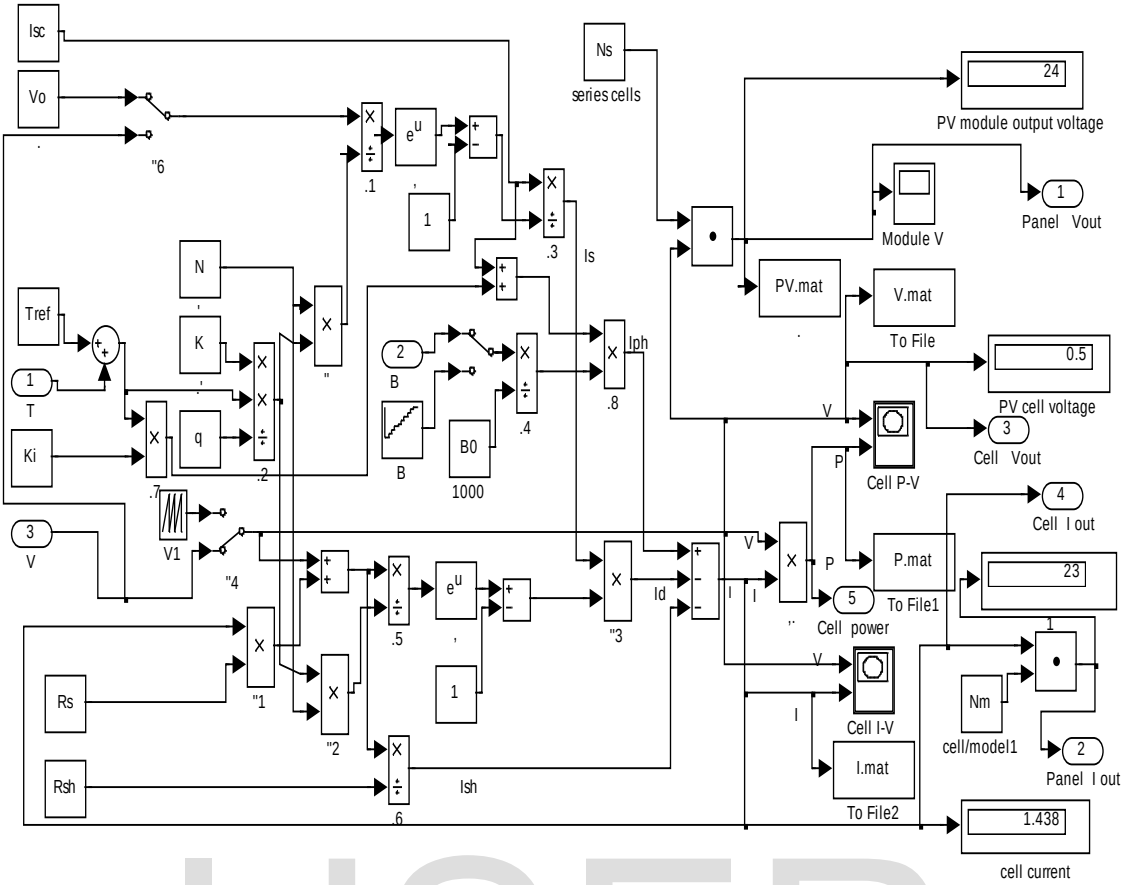

Fig. 5 (a) PV cell (module) Simulink subsystem model [25].

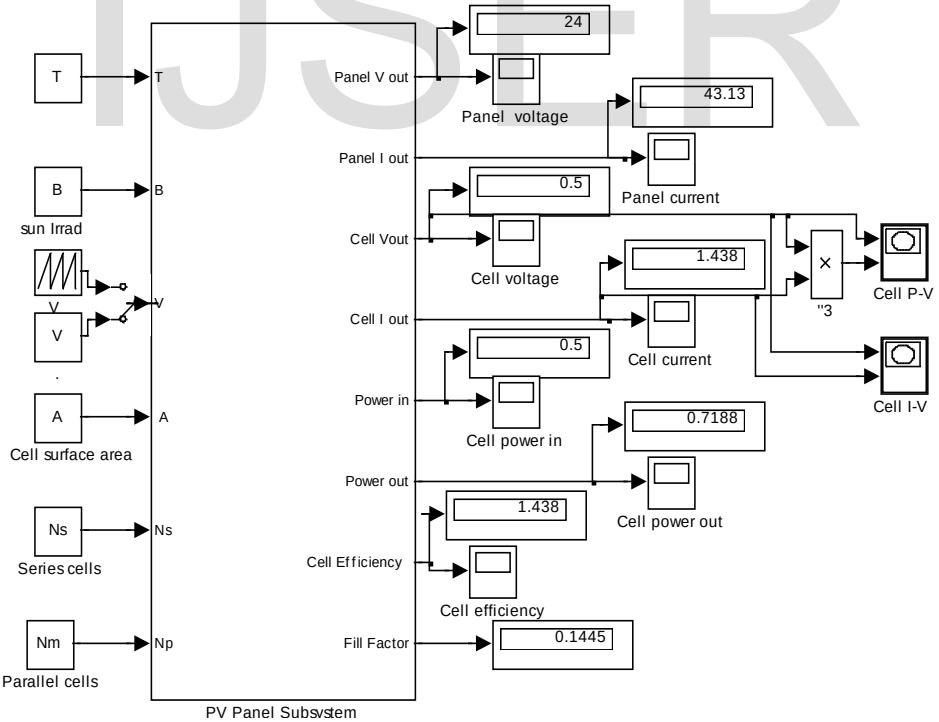

Fig. 5 (d) Generalized PV Cell(module) Simulink model [25]

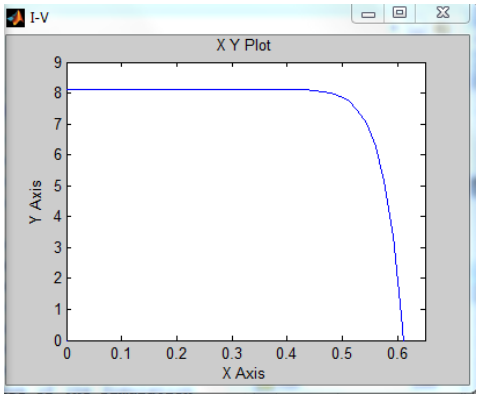

Fig. 5 (c) V-I Characteristics for β=1000, and T=25

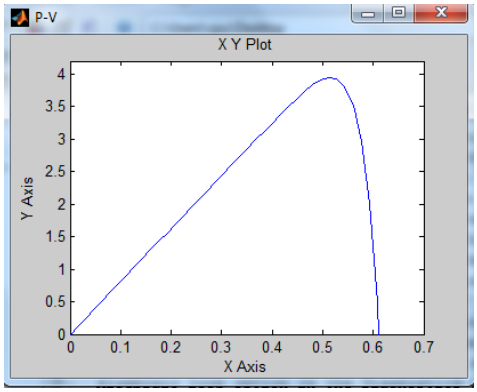

Fig. 5 (d) P-V Characteristics for β=1000, and T=25

2.3.2 DC/DC Converter subsystem modeling

Power converters can be classified intro three main types; step-up, step-down and step up and down. Most used and simple to model and simulate DC/DC converter include *Boost, Buck and buck-boost converters*. [24-25]. In this paper step-down DC/DC *Buck converters* is used. In [24], different models of *Buck* converter are derived, developed in Simulink and tested, including Buck converter circuit diagram shown in Fig. 6(a) and Simulink sub-model and masks shown in Fig. 6 (b)(c), also In [24] generalized Photovoltaic panel-Converter (PVPC) system Simulink model, shown in Fig. 6(d), is developed by integration both PV panel and converters subsystems sub-models resulting in model shown in Fig. 6(e). These Fig. show the outputs of both PVPC subsystems when tested for defined parameters listed in Table-1 including duty cycle of D=0.5. Duty cycle is the ratio of output voltage to input voltage is given by Eq.(40):

$$\frac{V_{out}}{V_{in}} = D = \frac{I_{in}}{I_{out}} \Rightarrow V_{out} = D * V_{in} \Leftrightarrow D = \frac{T_{on}}{T_{on} + T_{off}} \quad (40)$$

Where: I_{out} and I_{in}, : the output and input currents. D : the duty ratio (cycle) and defined as the ratio of the ON time of the switch to the total switching period. In this paper, the PWM generator is assumed as ideal gain system, the duty cycle of the PWM output will be multiplied with gain $K_V = K_D$, This equation shows that the output voltage of buck converter is lower than the input voltage; hence, the duty cycle is always less than 1.

2.3.3 Generalized Photovoltaic Panel–Converter (PVPC) subsystem model

Based on presented Simulink two sub-models of SEMRP system, PV panel subsystem and DC/DC converter subsystem , a generalized system model of PVPC system can be proposed and in generalize SEMRP system model shown in Fig. 6 (d)(e)

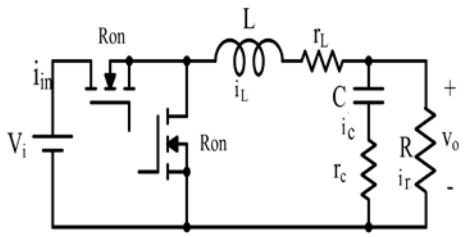

Fig. 3(a) Buck converter circuit diagram[24]

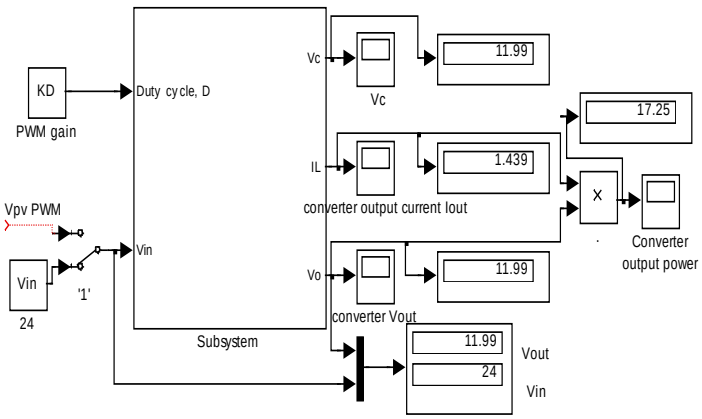

Fig. 3 (b) Buck converter Simulink model, based on refined math model[24]

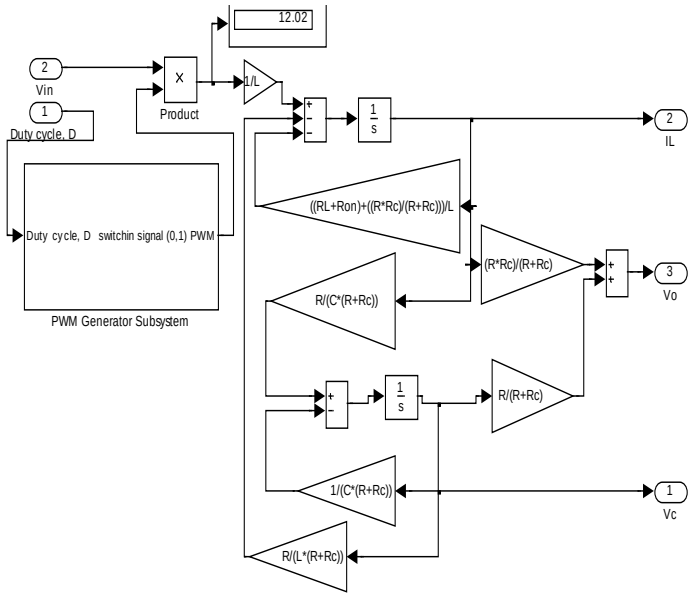

Fig. 6 (c) Buck converter subsystems model [24]

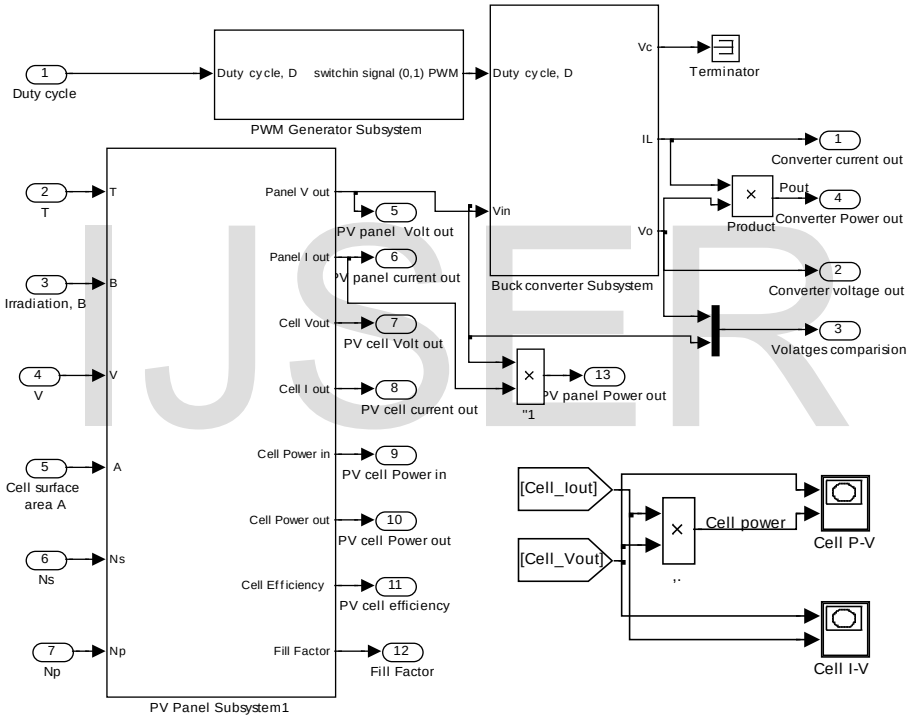

Fig. 6 (e) Generalized PVPC system sub-models consisting of three subsystems; PV panel, converter and PWM sub-models

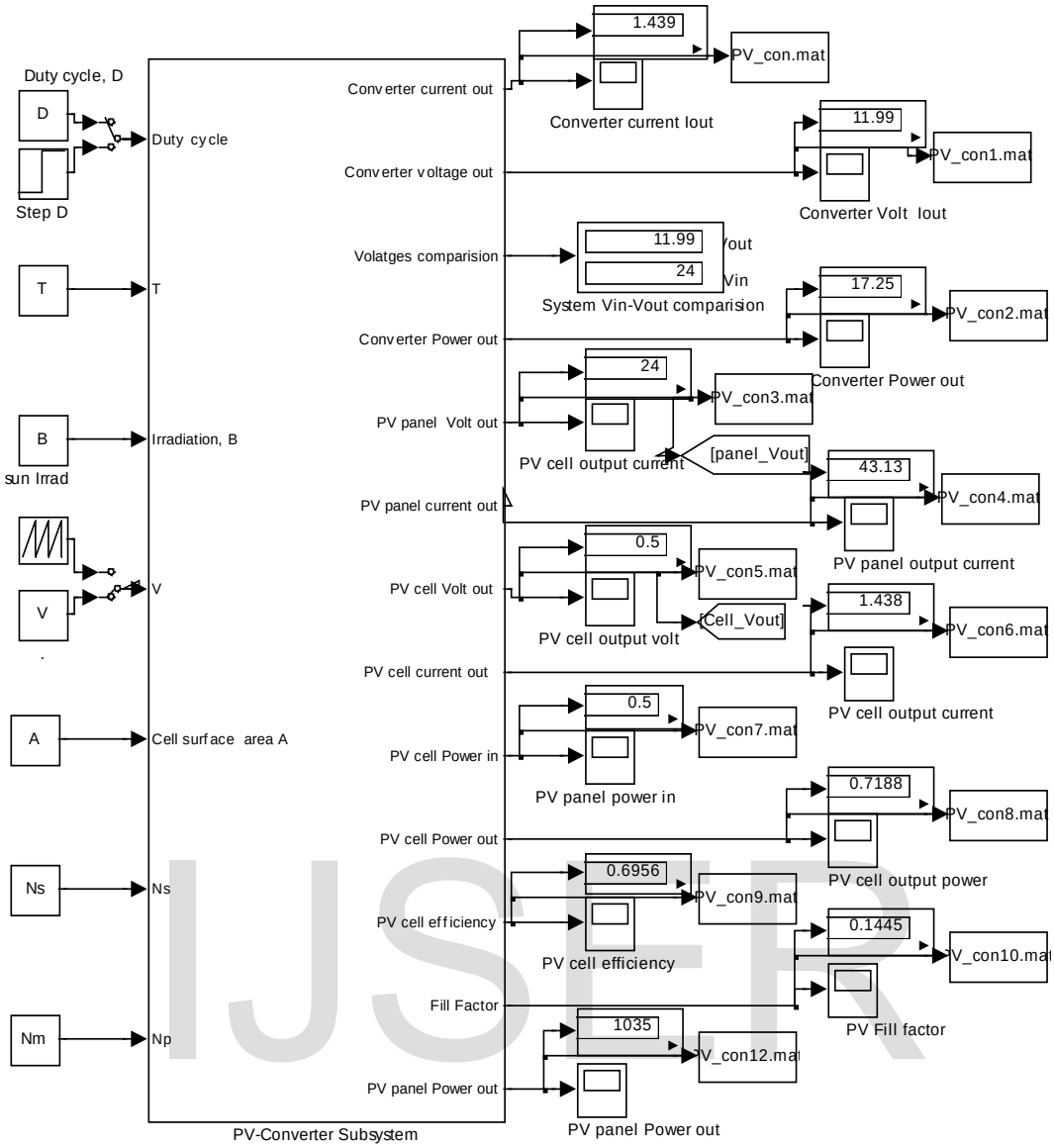

Fig. 6 (d) Generalized PVPC system model

2.4 Controller subsystem selection , modeling and design

Different control approaches can be proposed to control the overall SEMRP system output performance in terms of output speed, as well as, controlling output characteristics and performance of PVPC subsystem to meet desired output voltage or current under input working operating conditions.

PI controller: because of its simplicity and ease of design, PI controller is widely used in variable *speed* applications and *current* regulation, in this paper PI controller is selected for achieving desired outputs characteristics of PVPC subsystem and meeting desired output speed of overall SEMRP system, where Different PI controllers configurations are to be applied to control the PVPC subsystem and overall SEMRP system to achieve desired outputs of speed, voltage and load currents for particular SEMRP system application, it is important to notice that PI controller can be replace with PID or any other suitable control algorithm .

The *PI* controller transfer function in different forms is given by Eq.(41). The PI controller pole and zero will affect the response, mainly the PI zero given by; $Z_o=-K_I/K_P$, will inversely affect the response and should be canceled by prefilter, while maintaining the proportional gain (K_P), the prefilter transfer function is given by Eq.(42) , the placement of prefilter is shown on generalized model.

$$G_{PI}(s)=K_P+\frac{K_I}{s}=\frac{(K_P s+K_I)}{s}=\frac{K_P\left(s+\frac{K_I}{K_P}\right)}{s}= \quad (41)$$

$$=\frac{K_P(s+Z_o)}{s}=G_{PI}(s)=K_{PI}*\frac{(T_I s+1)}{T_I s}=K_{PI}*\left(1+\frac{1}{T_I s}\right)$$

$$G_{Prefilter}(s)=\frac{Z_O}{(s+Z_O)}=\frac{Z_{PI}}{(s+Z_{PI})} \quad (42)$$

PI controller with deadbeat response design, Deadbeat response means the response that proceeds rapidly to the desired level and holds at that level with minimal overshoot, The characteristics of deadbeat response include; Zero steady state error, Fast response, (short rise time and

settling time) and minimal undershoot, ±2% error band [14-15] [28], Controller with deadbeat response design is described and designed in details in [14]. In [15] a MATLAB built-in function to calculate desired deadbeat parameters including K_{PI} , Z_{PI} is designed and proposed.

3. Proposed generalized Solar Electric Mobile Robotic Platform (SEMRP) system model

Integrating all sub-models of all subsystems; particularly PV panel subsystem ,DC/DC buck converters subsystem, mobile platform subsystem, controller subsystem and load torque subsystem shown in Fig.s 3,4,5,6, will result in generalized SEMRP system model shown in Fig. 7(a), another generalized model can be proposed and shown in Fig. 7 (a) (in next section). *The inputs* to the first model are operating conditions of PV panel; irradiation β, working temperature T, PV panel-array construction including series N_s and parallel N_m cells and cell surface area A. The outputs of this model are numerical visual data, graphical data and output response curves of PV panel, converter and platform subsystems including; output linear speed, current, torque, acceleration, PV panel output current, volt, V-I and P-V Characteristics, finally, DC/DC converter output current and voltage. The generalized SEMRP system model is supported with different control algorithms including PID,PD,PI, PI with deadbeat response to control the mobile platform speed and performance, and can be modified to include any other control algorithm, also, also this model can be modified to include other control approaches to control PVPC subsystem outputs to match load requirements according to control approaches proposed in[25] including voltage and current control of PVPC subsystem to match platform voltage and current requirements

4. Testing and analysis

The proposed model works by defining the input operating condition and cells construction, based on this, the solar panel will generate corresponding output voltage , the DC/DC buck converter will reduce the input from PV panel voltage to platform voltage (*e.g 12* Volts) according to duty cycle D , the resulted from PVPC subsystem volts are fed to mobile platform for motion, finally, the selected and designed controller is used to control the performance of mobile platform to meet desired response and desired output speed.

*Testing the proposed generalized mode*l for desired output speed of 0.5 m/s for SEMRP subsystems parameters defined in Table-1, and under PV panel operating conditions of irradiation $\beta=200$, and $T=50$ and number of series $N_s=48$ and parallel $N_m= 30$, cell surface area $A=0.0025\ m^2$, and by applying PI controller with deadbeat response design, using methodology discussed in [14] and MATLAB built-in function designed in [15], with PI speed controller, will result in maximum output numerical visual and graphical output readings that allow designer to have the maximum data to select, design, integrate, tested and analyze the overall SEMRP system and each subsystem, these data output are listed in Table-2 and shown in Fig. 7(a)(b)(c), including PV panel currents of *41.01 A*, and voltage of *24 V*, Converter's output voltage of *12.01 V* , PV panel V-I and P-V Characteristics shown in Fig. 7(e)(f) , and Converter outputs current, voltages responses shown in Fig. 7 (g) , finally platform output linear speed of *0.5 m/s* and responses shown in Fig. 7(h), as well as platform torque, current and acceleration shown in Fig. 7(i)

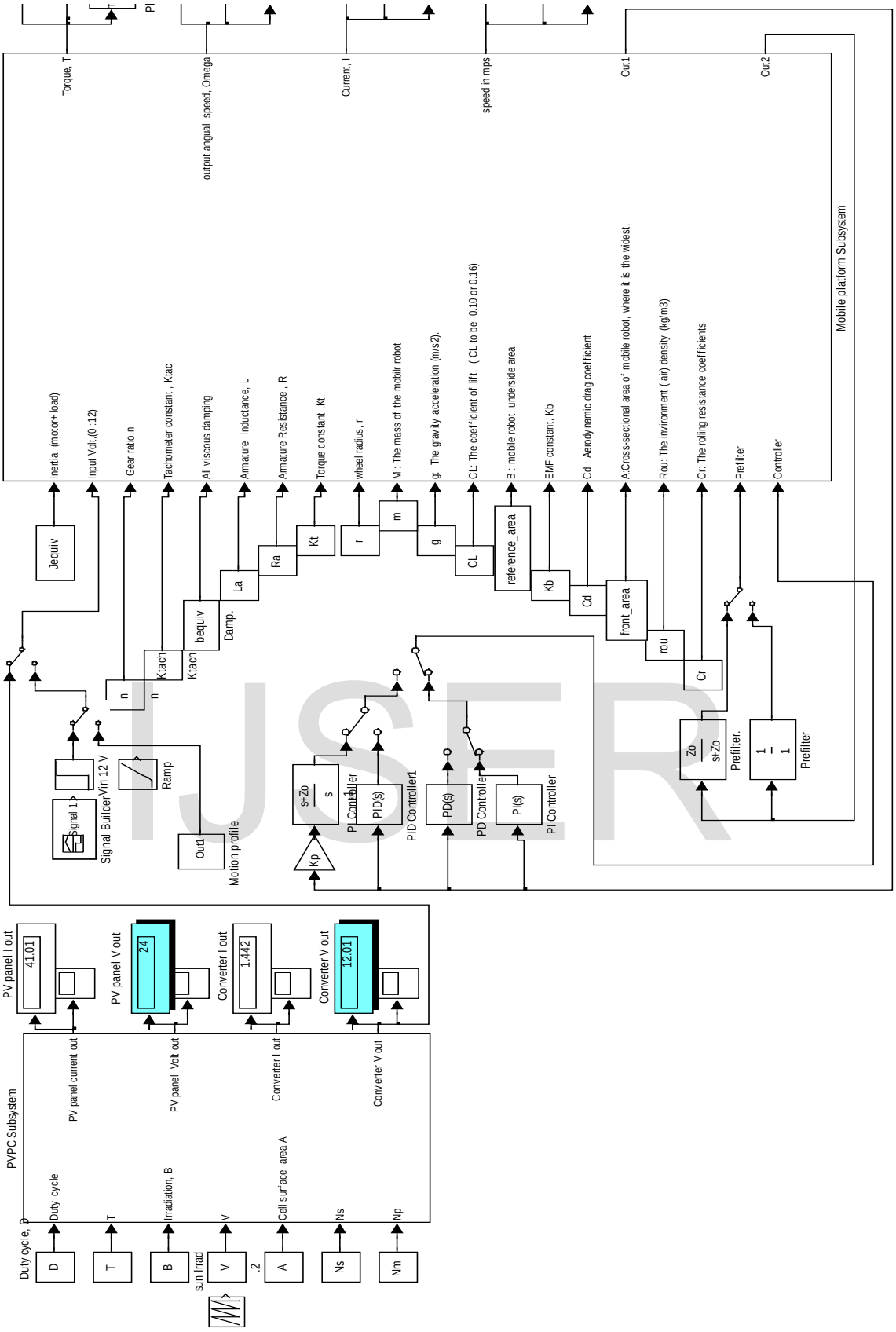

Fig. 7(a) Generalized Simulink model of SEMRP system

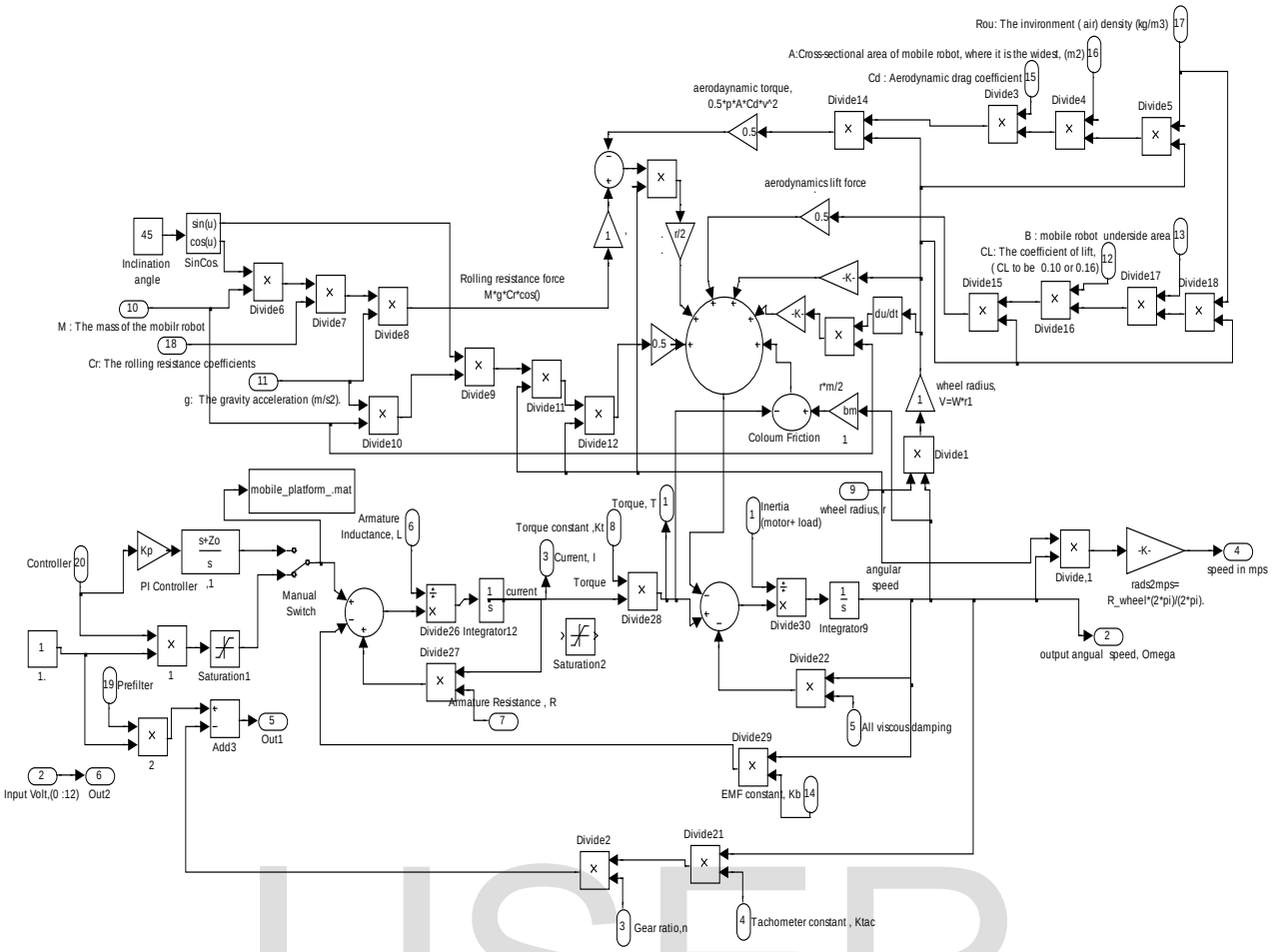

Fig. 7(b) Sub-model of DC machine with load torques

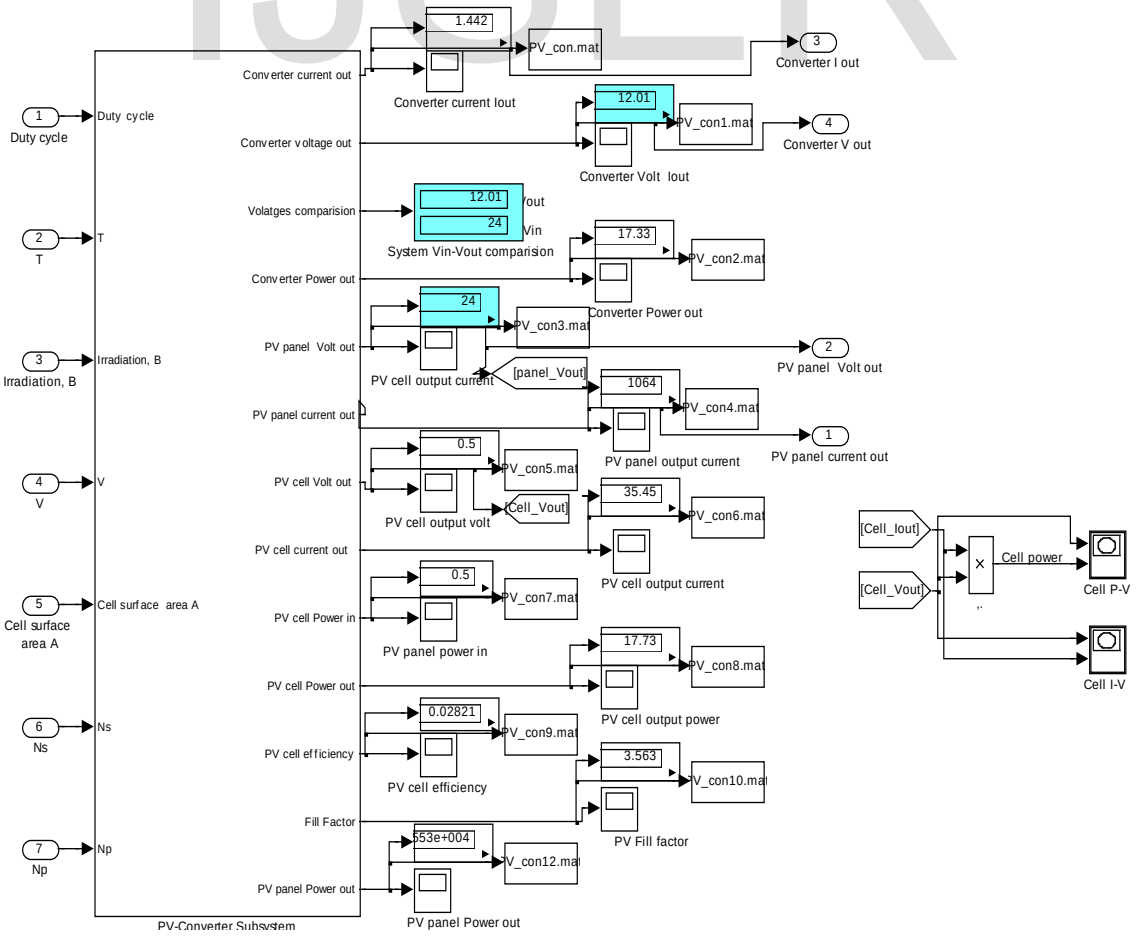

Fig. 7(c) Both subsystems of PVPC system models united in One sub-model

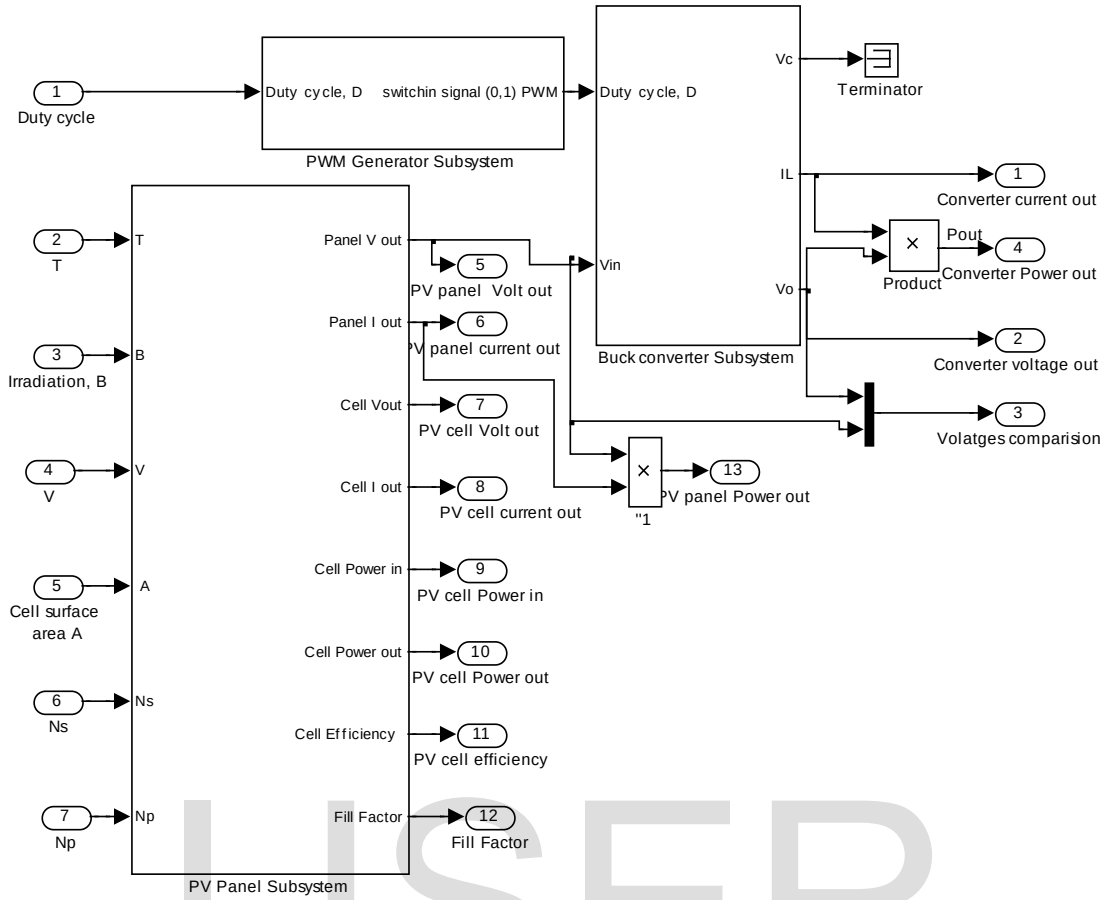

Fig. 7(d) Three sub-models of PVPC subsystem; panel, converter and PWM sub-models

Table 2 Simulation results of each subsystem and whole system

PVPC system inputs		PV cell outputs		PV Panel outputs		Converter outputs		SEMRP outputs	
β	200	Voltage	0.5 V	Voltage	24 V	Voltage	11.99 V	Linear Speed	0.5
T	50	Current	1.438 A	Current	43.134A	Current	1.439 A	Angular. Speed.	6.65
D	0.5	Fill factor	0.1445			Power out	17.25	motor Torque	7.021
A	0.0025	Power out	0.7188					Current	5.909
Ns	48	Power in	0.5						
Np	30	Efficiency	0.6956						

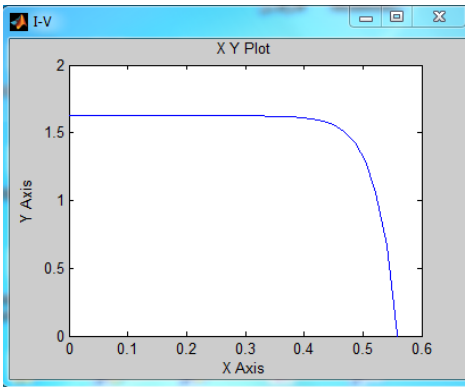

Fig. 7 (e) V-I Characteristics for β=200, and T=50

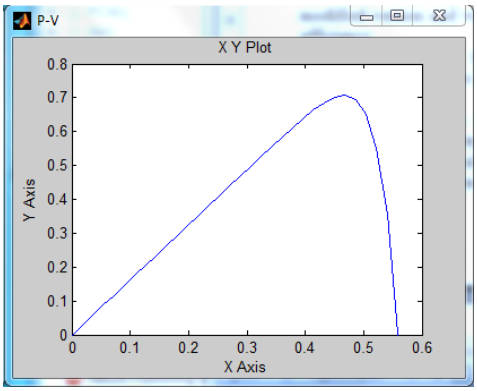

Fig. 7 (f) P-V Characteristics for β=200, and T=50

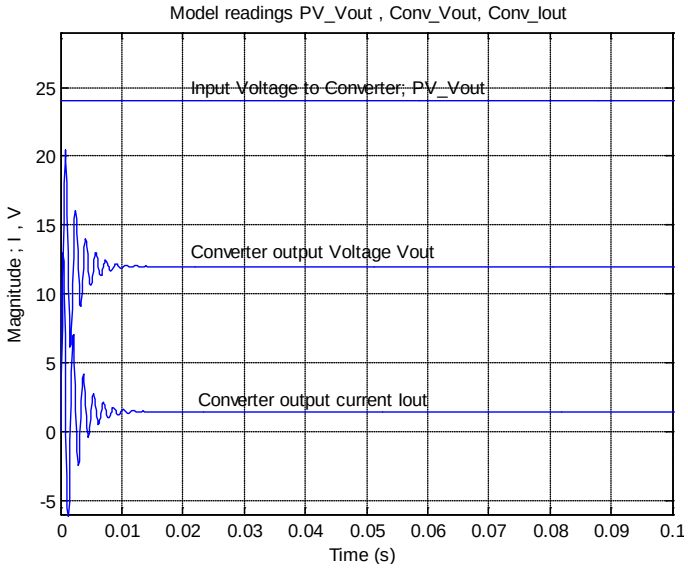

Fig. 7 (g) Inputs-outputs data of DC/DC Converter subsystem

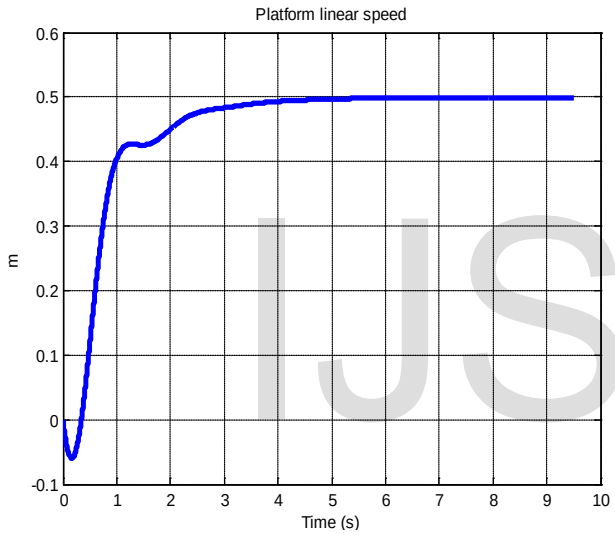

Fig. 7 (h) platform's output linear speed vs. time response

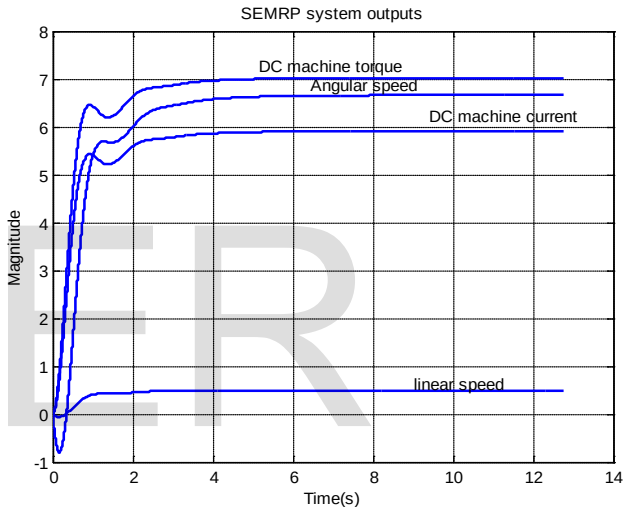

Fig. 7 (i) platform's output current, torque, speed, acceleration vs. time responses

4.1 Controller selection and design for specific purpose

The proposed generalized model can be modified to include different control algorithms to control PVPC subsystem performance and output characteristics, including controlling output current to match load-current, controlling output voltage to match load-voltage , controlling both output voltage and current to meet load requirements. In [25] different control approaches are applied and tested to control the performance and characteristics of the PVPC subsystem. In this paper controlling both PVPC subsystem current and voltage to meet load-platform desired voltage and current is to be applied, while achieving desired output speed using PI controller

4.2 Controlling both PVPC subsystem current and voltage to meet SEMRP load-platform system desired voltage and current, while achieving desired output speed.

The proposed control approach of the overall SEMRP system will have the configurations shown in Fig. 8 (a). PI controller and with prefilter and deadbeat response design, are used to control the mobile platform output linear speed to meet 0.5 m/s and 1 m/s, two control approaches are used to current and voltage control to meet desired platform load-current and voltage.

Matching load-platform desired current ; as shown in Fig. 8 (c) the comparison between load's and converter's currents is used to match the both currents, where load-platform current I_{load} is fedback to converter and compared with the converter output current I_{conv}, the difference is used to match the desired output platform current, according to the duty cycle D.

Controlling the converter's output voltage to meet desired platform voltage: *as* shown in Fig. 8 (b), The desired

converter output voltage and the converter actual output voltage are compared to calculate the error signal, used by PI controller to drive the converter switch according to the calculated duty cycle to meet platform voltage**,** The duty cycle *D* cycle is calculated automatically, as the ratio of converter's voltage to desired output voltage, and given by Eq.(43).

$$D = \frac{V_{Conv\_\_out\_desired}}{V_{Panel\_out}} \quad (43)$$

Testing the proposed model for desired converters output voltage ,$V_{out\_desired}$= *12 V* and desired linear speed of 1 m/s, at irradiation β= *200* and temperature *T=75*, for SEMRP system parameters values defined in table-1, will result in liner speed of1 m/s and currents, torque and acceleration shown in Fig. 8 (d)(e), and matching all currents (load-platform current, converter output current) to have the value of *10.45 A*, as well as, matching all volts to be *12 V*. Also, running the model, will result in all data required to analyze the SEMRP system performance and outputs characteristics, including converter output volts of *12* V, PV panel output voltage of *24* V, and duty cycle of D=*0.5* ,and I-V, and P-V characteristics, these values and other are numerically shown in Fig. 8 (a), the plots of PV panel output voltage, converter output voltage and converter output current are shown in Fig. 8 (d), the control signal is shown in Fig. 8 (e).

The proposed model can be modified to include PI current controller, where converter output current and DC motor armature current are compared and the different is used by PI current controller to control and ensure that the required load-platform current is met, the proposed control approach is shown in Fig. 8(f), running this model will result in same outputs shown in Fig. 8(c)(d)(e)(f)

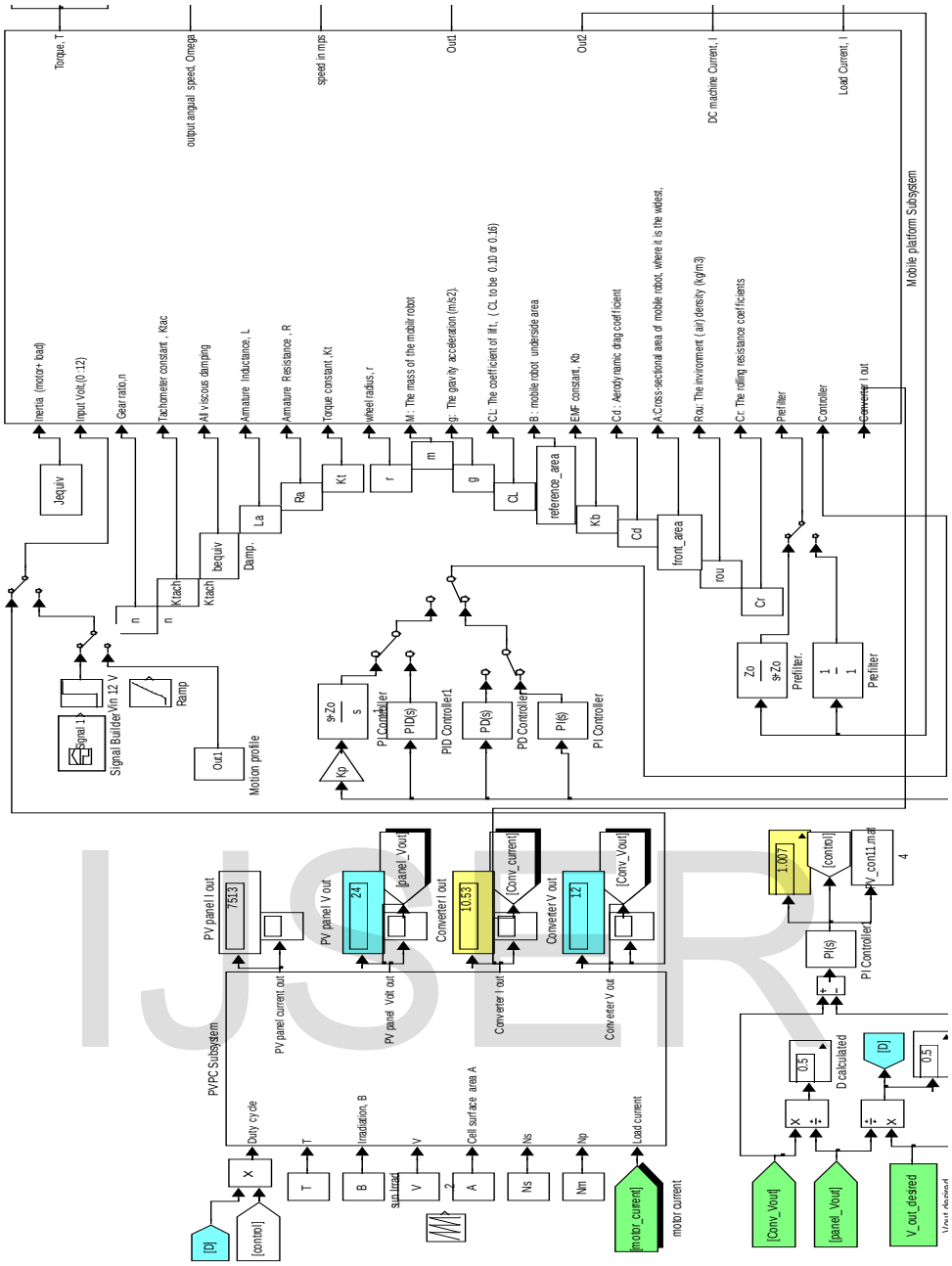

Fig. 8(a) proposed control approach for Controlling both PVPC subsystem current and voltage to meet SEMRP load-platform system desired voltage and current.

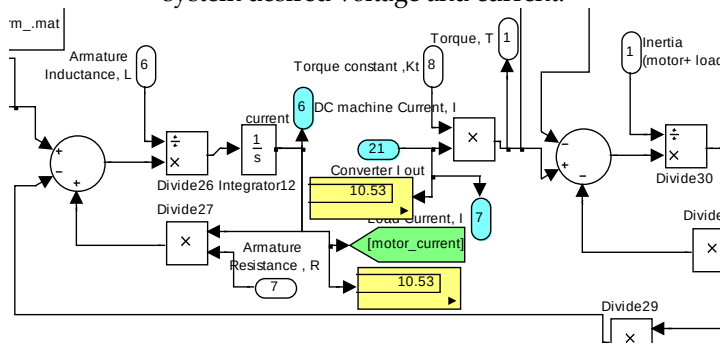

Fig. 8 (b) a part of DC machine subsystem showing platform and converter currents

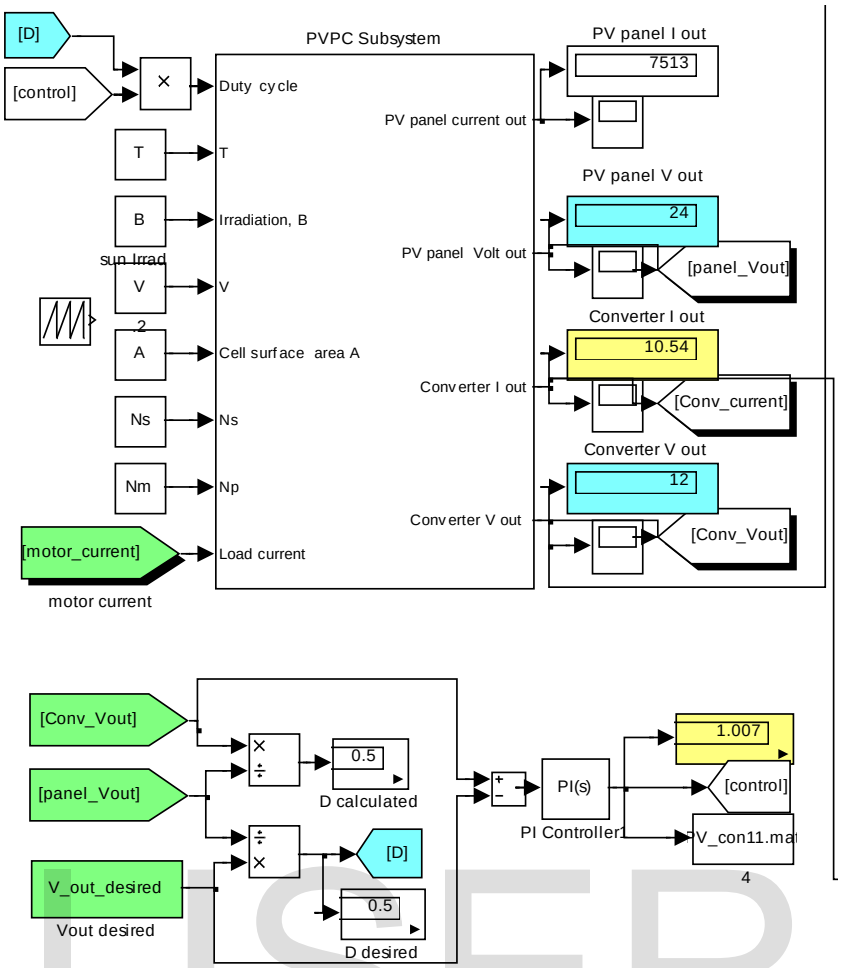

Fig. 8 (c) a part of DC machine subsystem showing platform and converter currents

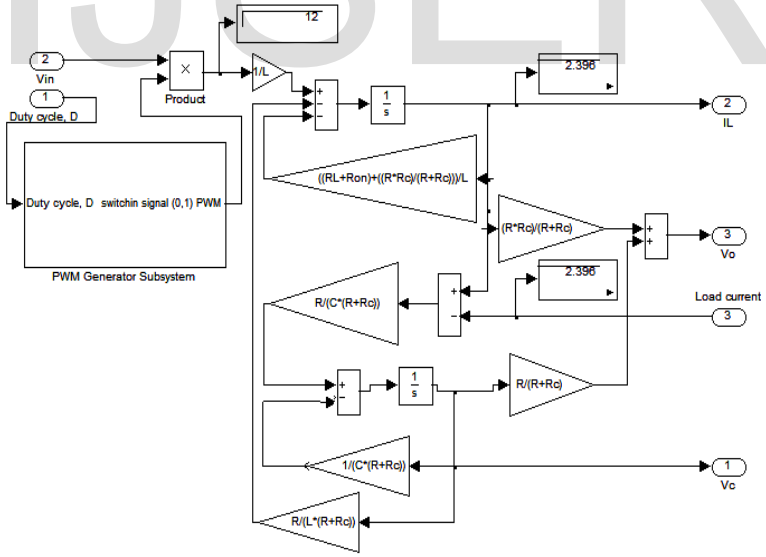

Fig. 8 (c) Comparing load-platform and converters currents to match load current

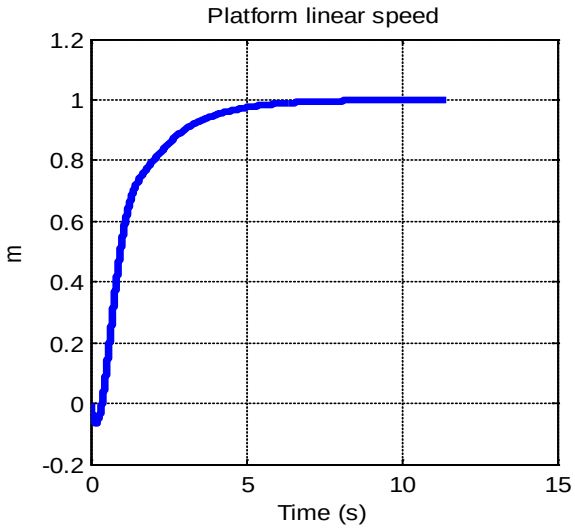

Fig. 8 (d) platform output linear speed

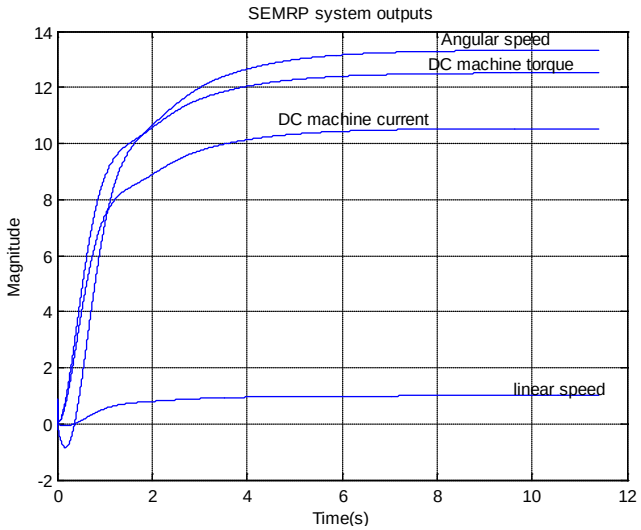

Fig. 8 (d) platform output speed, current , torque and acceleration VS time

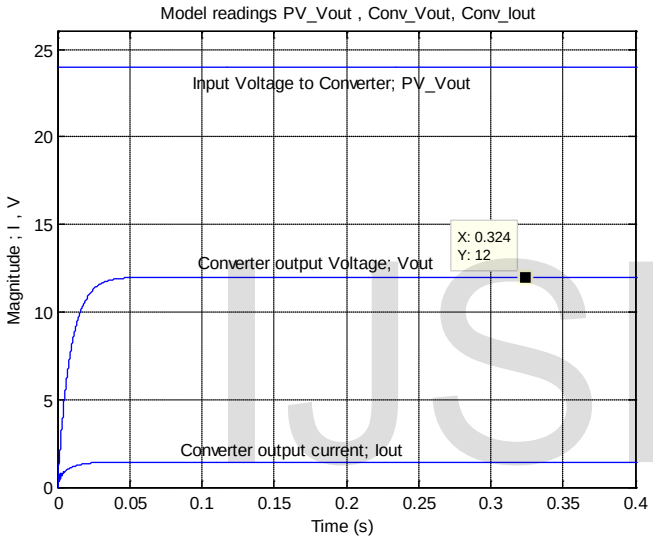

Fig. 8 (e) PVPC subsystem output readings ;voltage, converter output voltage and current

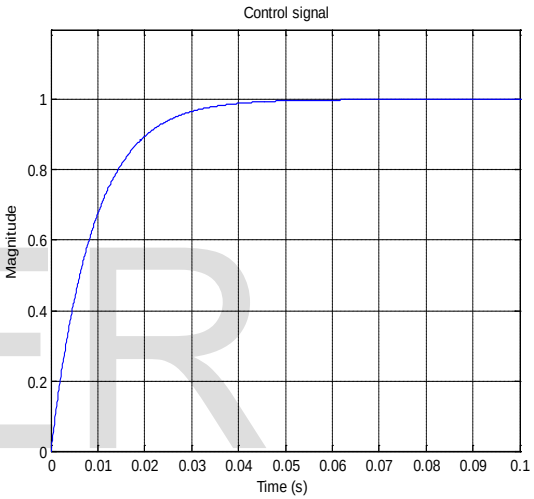

Fig. 8 (f) Control signal of PI controller

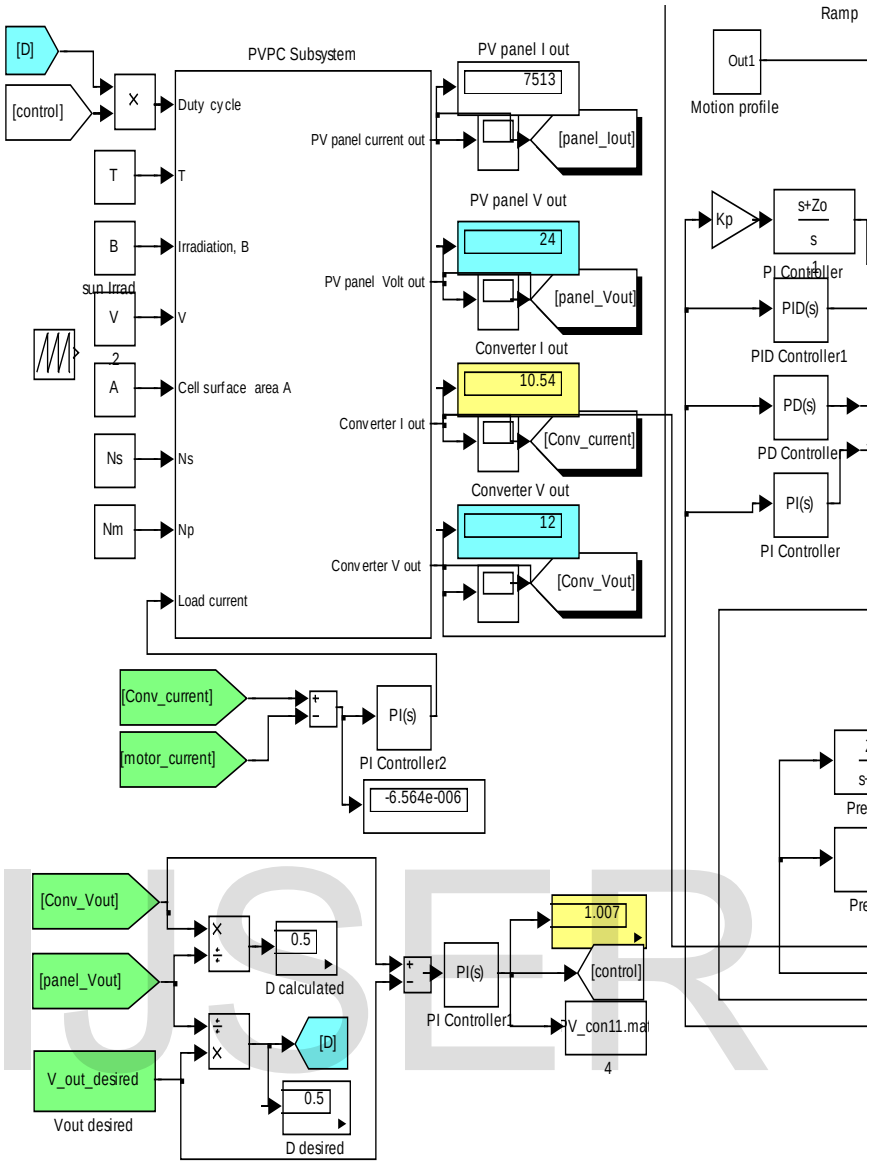

Fig. 8 (f) a part of generalized model showing control approaches of PVPC subsystem, using two separate PI current and voltage controllers .

4.3 Matching Photovoltaic Panel–Converter (PVPC) subsystem' current with platform's-load's current while achieving desired output speed.

The proposed control approach and the overall SEMRP system will have the configurations shown in Fig. 9(a). PI controller with prefilter and deadbeat response design, are used to control the mobile platform output speed, the PV panel subsystem is given as a function of $(V,I_{load}) = f(V,G,T)$, with input current, irradiation and working temperature , in the proposed load-current control approach the platform armature current is fed to PV panel and used to generate the output voltage and current of PV panel- converter subsystem. That will be fed to DC machine to generate desire torque to overcome load torque.

Testing the proposed model shown in Fig. 7 (a), by applying PI Controller with deadbeat response design, for SEMRP system with all subsystems' parameters defined in tablel including duty cycle of D=*0.5*, under operating conditions of PV panel; irradiation β=*200*, and *T=50* for desired output linear speed of 1 m/s, and PVPC subsystem' output voltage of *12 V*. will result in match

desired load-platform current to overcome load-torque and in all, numerical visual and graphical data required, (shown in Fig. 9(a)(b)(c)), as well as, output platform's linear speed of 0.9994 m/s , platform-load's current of 17.17 A, that is equal to converter output current of 17.17 A , and converter's output volt of *12* V, for PV panel output voltage of *24* V, and finally, V-I and P-V Characteristics of PV panel shown in Fig. 9(e)(f).

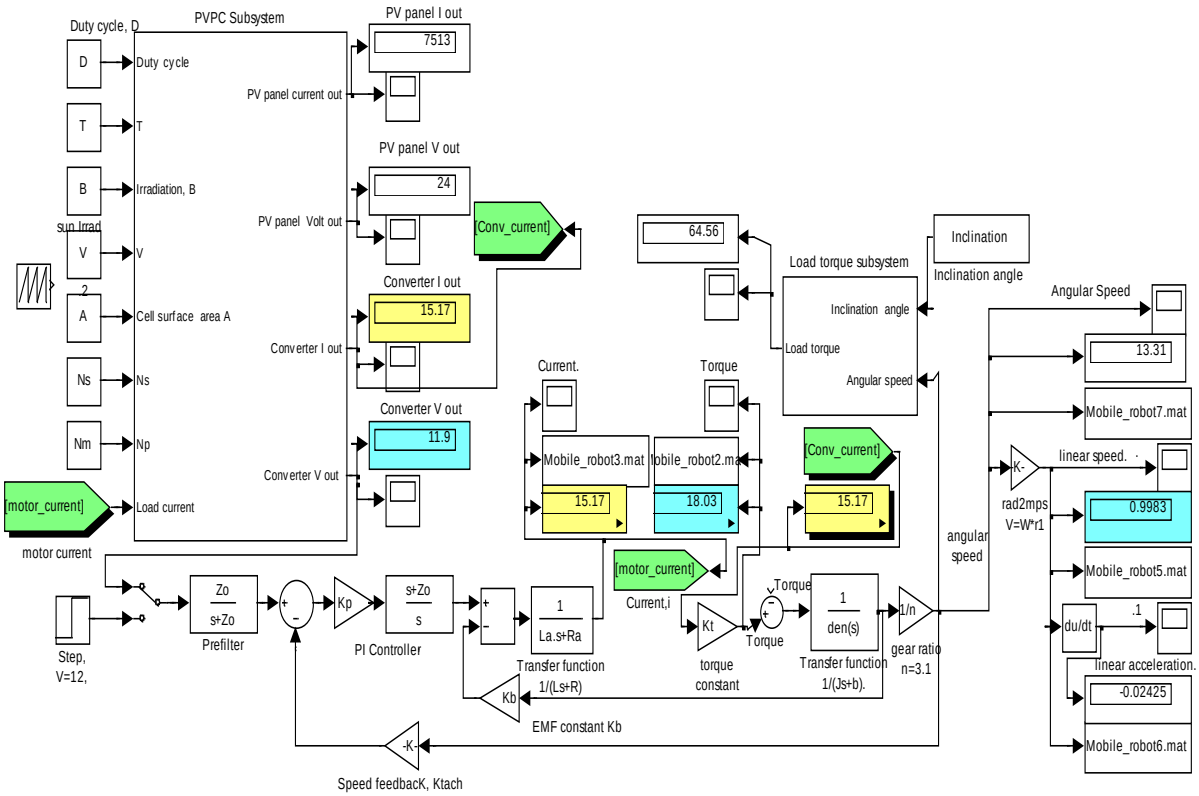

Fig. 9(a) proposed current control approach using second generalized model

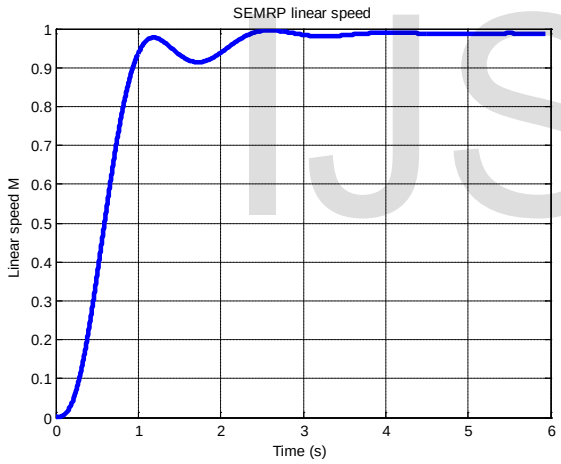

Fig. 9(b) SEMRP system output linear speed VS time applying currents comparison and PI controller with deadbeat response

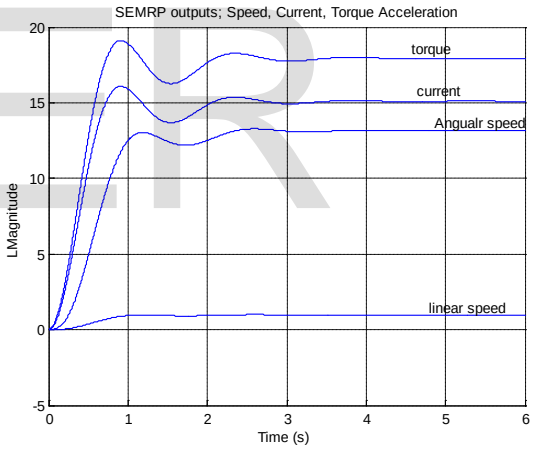

Fig. 9(c) SEMRP system output current, speed, torque and angular acceleration all VS time applying currents comparison and PI with deadbeat response

4.4 PI Controller for only speed performance control of SEMRP system in direct-coupling to the PVPC subsystem.

The overall SEMRP system will have the configurations shown in Fig. 10(a). In the proposed model, PI controller with deadbeat response is used to control the mobile platform output speed, no control is applied to control the PVPC subsystem output characteristics and performance.

Applying PI Controller with deadbeat response design, for subsystems parameters defined in Tablel-1 , under same operating conditions of PV panel, will result in numerical visual and graphical data and response curves shown in Fig. 10(a)(b), including V-I and P-V Characteristics of PV panel shown in Fig. 7(d)(e), the simulation and response curves show that under the given input operating condition, the solar panel will generate 24 Volts, the DC/DC buck converter will reduce the input from PV panel voltage to almost *12* Volts according to duty cycle of 0.5 , the resulted from PVPC subsystem *12* volts are fed to mobile platform to move, and PI controller with prefilter are used to control the performance of mobile platform to meet deadbeat response and meet desired 0.5 m/s output, a soft tuning of deadbeat controller parameters will soften the response.

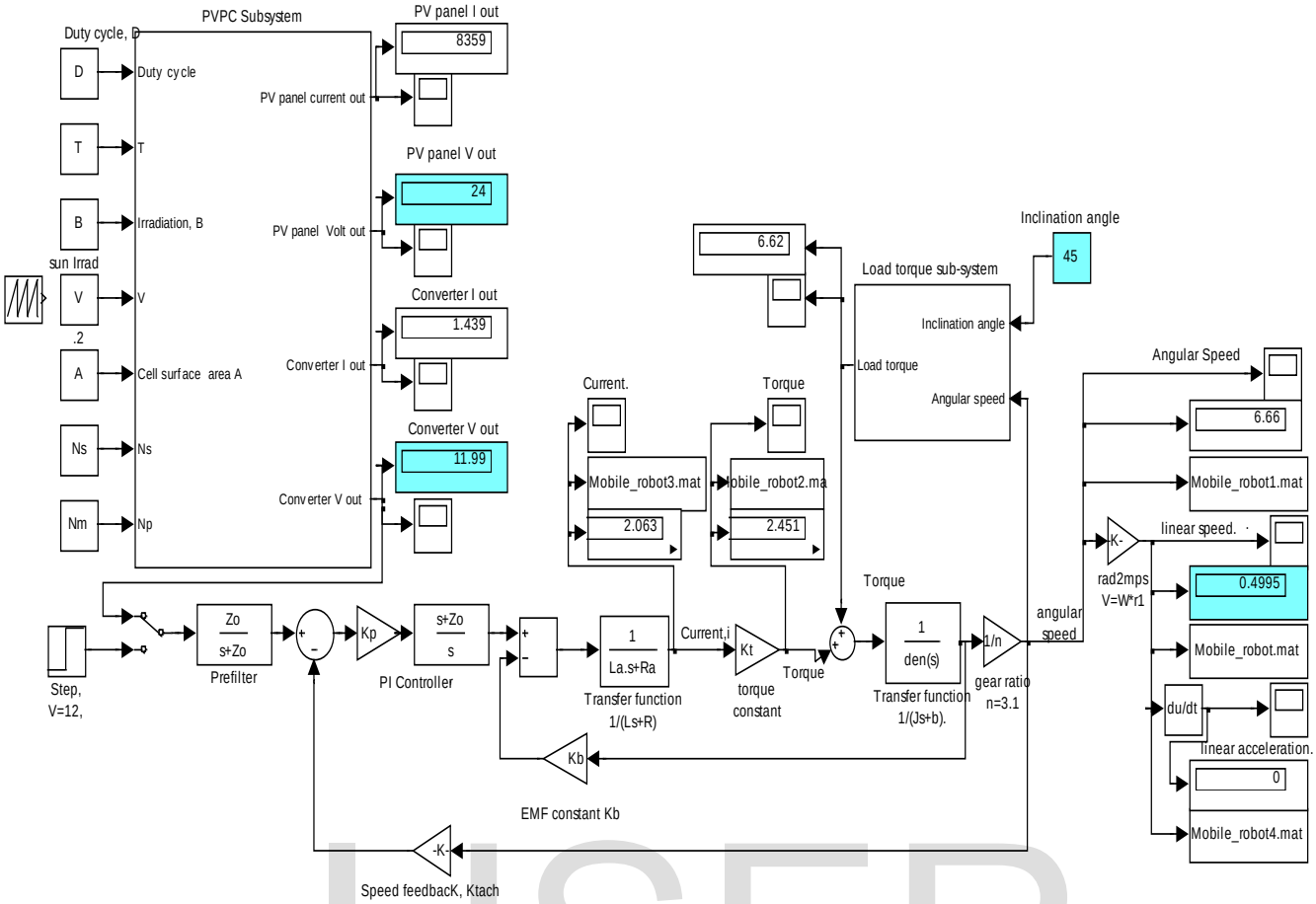

Fig. 10(a) proposed model of SEMRP system control applying PI with deadbeat

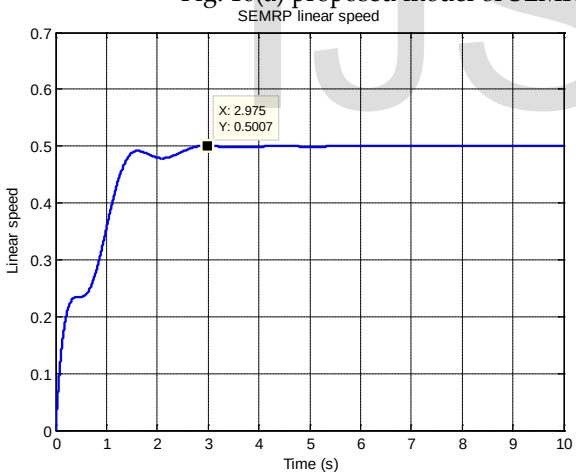

Fig. 10(d) SEMRP system speed VS time applying PI with deadbeat

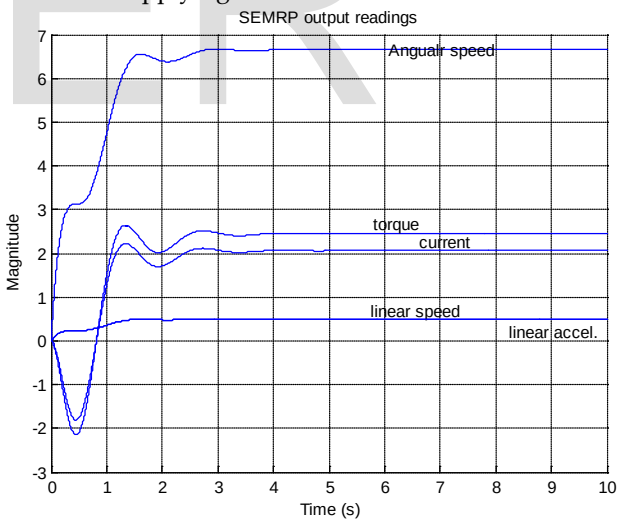

Fig. 10(e) SEMRP system output current, speed, torque and angular acceleration all VS time applying PI with deadbeat response

5. CONCLUSIONS

A generalized and refined model for Mechatronics design of Solar Electric Mobile Robotic Platforms (SEMRP) systems is proposed and tested, the proposed model consists of five main subsystems' sub-models, and is developed to allow designer to have the maximum output data to design, tested and analyze the overall SEMRP system and each subsystem, for desired overall and/or either subsystem's outputs under various PV subsystem operating conditions, to meet particular SEMRP system requirements and performance. the whole SEMRP system model and each subsystems model, are tested, analyzed and evaluated for desired system requirements and performance in Matlab/Simulink, the obtained results show the simplicity, accuracy and applicability of the presented models in Mechatronics design of SEMRP system

applications, as well as, for application in educational process.

Table 1 Nomenclature and nominal characteristic of SEMRP subsystems

	DC machine parameters
V_{in}=12 V	Input voltage to **DC machine**
K_t=1.188 Nm/A	Motor torque constant
R_a = 0.156 Ω	Motor armature Resistance
L_a=0.82 MH	Motor armature Inductance,
J_m=0.271 kg.m²	Geared-Motor Inertia
b_m=0.271 N.m.s	Viscous damping
K_b=1.185 rad/s/V	Back EMF constant,
n=1	Gear ratio
r=0.075 m,	Wheel radius
J_{equiv} kg.m²	The total equivalent inertia,
b_{equiv} N.m.s	The total equivalent damping,
L=0.4 m	The distance between wheels centers
K_{tac}=12/6.667=1.8 rad/s	Tachometer constant,
ω=speed/r, rad/s	=0.5/0.075=6.667 ,also 1/0.075=13.3333
T_{shaft}	The torque produced *by motor*
η	The transmission efficiency
T_{shaft}	The torque, produced by the driving motor
	Nominal values for Mobile platform
M,m, Kg	The mass of the mobile platform
C_d =0.80	Aerodynamic drag coefficient
C_L	The coefficient of lift, with values(C_L to be 0.10 or 0.16),
Cr=0.5	The rolling resistance coefficient
ρ , kg/m³	The air density at STP, ρ =1.25
a, m/s²	Platform linear Acceleration
G, m/s²	The gravity acceleration
N, m/s	The vehicle linear speed.
α , Rad	Road *slope* or the hill climbing angle
B	Mobile platform's reference area
L	lift,
A_f	Platforms frontal area
K_P	Proportional gain
K_I	Integral gain
Z_0	PI controller zero
P_m	The power available in the wheels of the vehicle.
T_{Total}	The total resistive torque, the torque of all acting forces.
	Solar cell parameters
Isc=8.13 A , 2.55 A , 3.8	The short-circuit current, at reference temp 25°C
I A	The output net current of PV cell (*the* PV *module current*)
I_{ph} A	The light-generated *photocurrent* at the nominal condition (25°C and 1000 W/m²),
E_g : =1.1	The band gap energy of the semiconductor
$V_t = KT / q$	The thermo voltage of cell. For array :($V_t = N_s KT / q$)
I_s ,A	The reverse saturation current of the diode or leakage current of the diode
Rs=0.001 Ohm	The series resistors of the PV cell, it they may be neglected to simplify the analysis.
Rsh=1000 Ohm	The shunt resistors of the PV cell
V	The voltage across the diode, output
q=1.6e-19 C	The electron charge
B_o=1000 W/m²	The Sun irradiation
β =B=200 W/m²	The irradiation on the device surface
Ki=0.0017 A/◦C	The cell's short circuit current temperature coefficient
Vo= 30.6/50 V	Open circuit voltage
Ns= 48 , 36	Series connections of cells in the given photovoltaic module
Nm= 1 , 30	Parallel connections of cells in the given photovoltaic module
K=1.38e-23 J/oK;	The Boltzmann's constant
N=1.2	The diode ideality factor, takes the value between 1 and 2
T= 50 Kelvin	Working temperature of the *p-n* junction
T_{ref}=273 Kelvin	The nominal reference temperature
	Buck converter parameters
C=300e-6; 40e-6 F	Capacitance
L=225e-6 ; .64e-6 H	Inductance
Rl=RL=7e-3	Inductor series DC resistance
rc= RC=100e-3	Capacitor equivalent series resistance, ESR of C ,
V_{in}= 24 V	Input voltage
R=8.33; 5 Ohm;	Resistance
Ron=1e-3;	Transistor ON resistance
KD=D= 0.5, 0.2,	Duty cycle

Tt=0.1 , 0.005	Low pass Prefilter time constant
V_L	Voltage across inductor
I_C	Current across Capacitor

REFERENCES

[1] Farhan A. Salem, Ahmad A. Mahfouz , A Proposed Approach to Mechatronics Design and Implementation Education-Oriented, Innovative Systems Design and Engineering , Vol.4, No.10, pp 12-39,2013.

[2] Stephen Se, David Lowe ,Jim Little, Mobile Robot Localization and Mapping with Uncertainty using Scale-Invariant Visual Landmarks, The International Journal of Robotics Research, Vol. 21, No. 8, August 2002, pp. 735-758,2002

[3] J. Borenstein, B. Everett, and L. Feng. Navigating Mobile Robots: Systems and Techniques. A. K. Peters Ltd, Wellesley, MA, 1996.

[4] A.J. Davison and D.W. Murray. Mobile robot localisation using active vision. In *Proceedings of Fifth European Conference on Computer Vision (ECCV'98) Volume II*, pages 809{825, Freiburg, Germany, June1998.

[5] H. Andreasson, A. Treptow, and T. Duckett. Localization for mobile robots using panoramic vision, local features and particle filter. In Proc. of the IEEE Int. Conf. on Robotics & Automation (ICRA), 2005..

[6] D. Brˇsˇci´c and H. Hashimoto. Comparison of robot localization methods using distributed and onboard laser range finders. In IEEE/ASME Int. Conf. on Advanced Intelligent Mechatronics, 2008.

[7] J. Borenstein,, H.R. Everett,, L. Feng,, and D. Wehe,Mobile Robot Positioning and Sensors and Techniques, *Invited paper for the Journal of Robotic Systems, Special Issue on Mobile Robots. Vol. 14 No. 4, pp. 231 – 249.*

[8] Barshan, B. and Durrant-Whyte, H.F., 1995, "Inertial Navigation Systems Mobile Robots." IEEE Transactions on Robotics and Automation, Vol. 11, No. 3, June, pp. 328-342.

[9] Borenstein, J., Everett, B., and Feng, L., 1996b, "*Navigating Mobile Robots: Systems and* Techniques.", A. K. Peters, Ltd., Wellesley, MA, ISBN 1-56881-058-X.

[10] PeLoTe Session,Mobile Robots for Search and Rescue, Proceedings of the 2005 IEEE International Workshop on Safety, Security and Rescue Robotics Kobe, Japan, June 2005.

[11] J. Kuhle, H. Roth, and N. Ruangpayoongsak, "mobile robotics and airships in a multi-robot team," *The 1st IFAC Symposium on Telematics Applications in Automation and Robotics*, Helsinki University of Technology, Finland, pp. 67-72, June 2004.

[12] Farhan A. Salem ,Dynamic and Kinematic Models and Control for Differential Drive Mobile Robots, International Journal of Current Engineering and Technology, Vol.3, No.2 (June 2013)

[13] Farhan A. Salem, Ahmad A. Mahfouz , A Proposed Approach to Mechatronics Design and Implementation Education-Oriented, Innovative Systems Design and Engineering , Vol.4, No.10, pp 12-39,2013.

[14] Farhan A. Salem, Refined modeling and control for Mechatronics design of mobile robotic platforms, Estonian Journal of Engineering, 19, 3, 212–238,2013.

[15] Farhan A. Salem, Mechatronics motion control design of electric machines for desired deadbeat response specifications, supported and verified by new MATLAB built-in function and Simulink model, submitted to European journal 2013 .

[16] Ahmad A. Mahfouz, Ayman A. Aly, Farhan A. Salem , Mechatronics Design of a Mobile Robot System, I.J. Intelligent Systems and Applications, 03, 23-36, 2013.

[17] Ahmad A. Mahfouz, Mohammed M. K., Farhan A. Salem , Modeling, Simulation and Dynamics Analysis Issues of Electric Motor, for Mechatronics Applications, Using Different Approaches and Verification by MATLAB/Simulink (I). *I.J. Intelligent Systems and Applications,pp39-57* ,05, 39-572013,

[18] Farhan A. Salem, mobile robot dynamics analysis and control ,VI Международная научно-практическая конференция , «Инженерные системы - 2013».

[19] Jaroslav Hanzel , Ladislav Jurišica , Marian Kľúčik , Anton Vitko , Matej Strigáč, Experimental mobile robotic system

[20] Bashir M. Y. Nouri , modeling and control of mobile robots, Proceeding of the First International Conference on Modeling,

Simulation and Applied Optimization, Sharjah, U.A.E. February 1-3, 2005.

[21] Wai Phyo Aung, Analysis on Modeling and Simulink of DC Motor and its Driving System Used for Wheeled Mobile Robot, World Academy of Science, Engineering and Technology 32 2007

[22] Mircea Niţulescu, solution for modeling and control in mobile robotics, control engineering and applied informatics -CEAI,, Vol. 9, No. 3;4, pp. 43-50, 2007

[23] Farhan A. Salem, 'Modeling and Simulation issues on Photovoltaic systems, for Mechatronics design of solar electric applications, IPASJ International Journal of Mechanical Engineering (IIJME),Volume 2, Issue 8, August 2014.

[24] Farhan A. Salem, New generalized Photovoltaic Panel-Converter system model for Mechatronics design of solar electric applications, IPASJ International Journal of Mechanical Engineering (IIJME),Volume 2, Issue 8, August 2014.

[25] Farhan A. Salem, Photovoltaic-Converter system, modeling and control issues for Mechatronics design of solar electric application, *I.J. Intelligent Systems and Applications*, 08,2014,

[26] Farhan A. Salem, Mechatronics Design of Motion Systems; Modeling, Control and Verification , International Journal of Mechanical & Mechatronics Engineering IJMME-IJENS Vol:13 No:02 , 2013.

[27] Farhan A. Salem, Dynamic Modeling, Simulation and Control of Electric Machines for Mechatronics Applications, international journal of control, automation and systems Vol.1 No.2, pp30-41, April, 2013.

[28] Richard C. Dorf and Robert H. Bishop, Modern Control Systems, Ninth Edition, Prentice-Hall Inc., New Jersey, 2001.

[29] Farhan A. Salem, Mechatronics Design of Solar Tracking System, International Journal of Current Engineering and Technology, Vol.3, No.2 (June 2013)